Electronic Supplementary Material (ESI) for Organic & Biomolecular Chemistry.

Table of Contents

- **General Remarks and Materials**

All chemicals those syntheses are not reported hereafter were purchased from commercial sources and used as received. Solvents were dried and stored over molecular sieves previously activated in an oven (450 °C overnight). Anhydrous CH_2Cl_2 for catalytic reactions was supplied by Fluka in Sureseal® bottles and used without any further purification. Column chromatography was performed on silica gel 60 (70-230 mesh). Melting points were measured with an Electrothermal apparatus and are uncorrected. NMR spectra were recorded on a Bruker 400 MHz and JEOL 600 MHz using solvents as internal standards (7.26 ppm for ^{1}H NMR and 77.00 ppm for ^{13}C NMR for $CDCl_3$). The terms m, s, d, t, q and quint represent multiplet, singlet, doublet, triplet, quadruplet and quintuplet respectively, and the term br means a broad signal. ^{13}C APT NMR spectra are reported for enynes **1** and corresponding products **2**. Exact masses were recorded on a LTQ ORBITRAP XL Thermo Mass Spectrometer (ESI source).

Materials: Targeted *N*-propargyl sulfonamides **1'** were synthesized in variable yields (70-88%) from commercial sulfonyl chlorides following typical protocols. Propargylamine/RSO_2Cl/TEA (1.0/1.2/2 equiv.), CH_2Cl_2 (0.2 M), r.t., 4 hours.[1] Calix[6]arene catalysts **A**, **B**, **C**$(AuCl)_2$ were synthesized according to a previously reported protocol.[2] Enynes **1a**-**b** were synthesized according to known procedures.[3]

- **Crystallographic Data**

Refinement additional details

A$(AuCl)_2$

Both tertbutyl moieties were found disordered over two sites, which were modelled respectively with 0.50-0.50 and 0.80-0.20 site occupancy factors. Two acetonitrile molecules were pinpointed in the asymmetric unit: the first one was fully occupied and interacted with calix[6]arene NH moiety, the latter one was partially occupied (50%) and DFIX, DANG, SIMU ad ISOR restraints were employed for the final refinement.

B$(AuCl)_2$

Tertbutyl and octyl moieties were found disordered over two distinct sites, which were modelled with 0.70-0.30 site occupancy factors. One H-bonded diethyl ether and three toluene molecules were located in the asymmetric unit, two of which were disordered over two sites (refined with 70:30 occupancies).

C$(AuCl)_2$

Both tertbutyl moieties were found disordered over two sites, which were both modelled with a 0.50-0.50 site occupancy factors. The octyl chain was found located over three different alternative orientation. The position of the one with the highest occupancy (50%) was mutually exclusive with a chloroform molecule (25% occupancy), while the remaining two were refined both with 0.25 site occupancy factor. The asymmetric unit comprised another partially occupied chloroform molecule (50% occupancy).

Asymmetric units

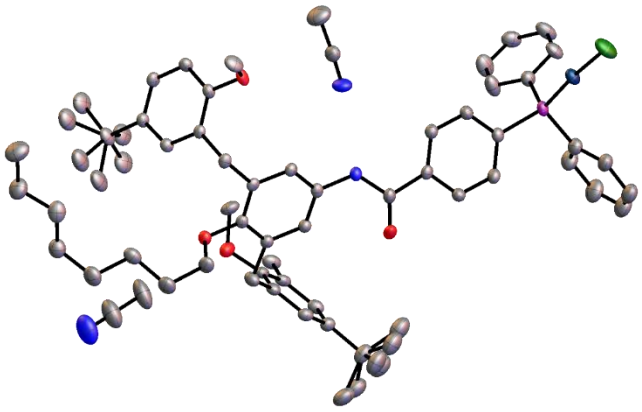

Figure S 1 Asymmetric unit view of **A**$(AuCl)_2$, thermal ellipsoids are plotted at 30% probability level (colour code: C, grey; O, red; N, blue; P, purple; Au, dark blue; Cl, green; hydrogen atoms are omitted for clarity). Two partially occupied acetonitrile molecule were modelled from residual electron density.

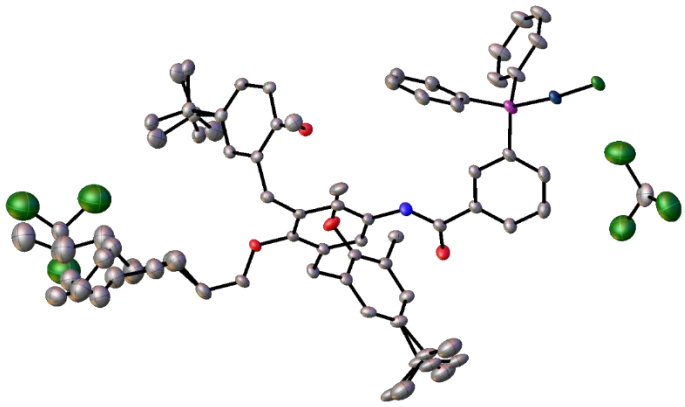

Figure S 2 Asymmetric unit view of **B**$(AuCl)_2$, thermal ellipsoids are plotted at 30% probability level (colour code: C, grey; O, red; N, blue; P, purple; Au, dark blue; Cl, green; hydrogen atoms are omitted for clarity). Two partially occupied chloroform molecules were modelled from residual electron density

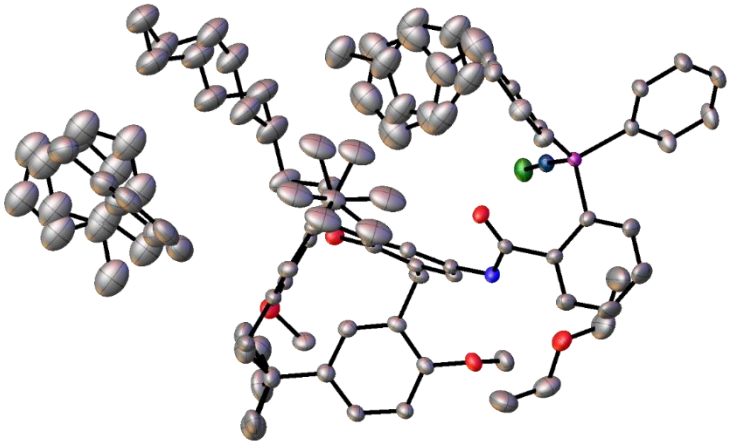

Figure S 3 Asymmetric unit view of **C**$(AuCl)_2$, thermal ellipsoids are plotted at 30% probability level (colour code: C, grey; O, red; N, blue; P, purple; Au, dark blue; Cl, green; hydrogen atoms are omitted for clarity). Three partially occupied toluene and one H-bondend diethyl ether molecules were modelled from residual electron density

Crystallographic tables

Table S1 Crystal data and structure refinement for **A**$(AuCl)_2$

Empirical formula	$C_{122}H_{145}Au_2Cl_2N_5O_8P_2$
Formula weight	2336.19
Temperature/K	200.00
Crystal system	triclinic
Space group	P-1
a/Å	12.0018(3)
b/Å	15.5165(4)
c/Å	17.7252(4)
α/°	68.278(2)
β/°	84.913(2)
γ/°	85.553(2)
Volume/Å^3	3050.85(14)
Z	1
ρ_{calc}g/cm^3	1.272
μ/mm^{-1}	2.525
F(000)	1198.0
Crystal size/mm^3	0.15 × 0.09 × 0.07
Radiation	Mo Kα (λ = 0.71073)
2Θ range for data collection/°	4.084 to 51.362
Index ranges	-14 ≤ h ≤ 14, -18 ≤ k ≤ 18, -21 ≤ l ≤ 21
Reflections collected	75557
Independent reflections	11536 [R_{int} = 0.0918, R_{sigma} = 0.0454]
Data/restraints/parameters	11536/209/710
Goodness-of-fit on F^2	1.072
Final R indexes [I>=2σ (I)]	R_1 = 0.0486, wR_2 = 0.1334
Final R indexes [all data]	R_1 = 0.0553, wR_2 = 0.1360
Largest diff. peak/hole / e Å^{-3}	1.98/-0.96

$R_1 = \Sigma||F_o|-|F_c||/\Sigma|F_o|$, $wR_2 = [\Sigma[w(F_o^2-F_c^2)^2]/\Sigma[w(F_o^2)^2]]^{½}$, $w = 1/[\sigma^2(F_o^2) + (aP)^2 + bP]$, where $P = [max(Fo^2,0) + 2Fc^2]/3$

Table S2 Crystal data and structure refinement for **B**$(AuCl)_2$

Empirical formula	$C_{117.5}H_{137.5}Au_2Cl_{6.5}N_2O_8P_2$
Formula weight	2392.08
Temperature/K	200.00
Crystal system	monoclinic
Space group	C2/c
a/Å	30.4353(6)
b/Å	15.4148(2)
c/Å	25.1048(4)
α/°	90
β/°	90.541(2)
γ/°	90
Volume/Å^3	11777.5(3)
Z	4
ρ_{calc}g/cm^3	1.349
μ/mm^{-1}	2.716
F(000)	4876.0
Crystal size/mm^3	0.1 × 0.03 × 0.03
Radiation	MoKα (λ = 0.71073)
2Θ range for data collection/°	3.384 to 51.362
Index ranges	-37 ≤ h ≤ 37, -18 ≤ k ≤ 18, -30 ≤ l ≤ 30
Reflections collected	115349
Independent reflections	11167 [R_{int} = 0.0631, R_{sigma} = 0.0272]
Data/restraints/parameters	11167/467/794
Goodness-of-fit on F^2	1.048
Final R indexes [I>=2σ (I)]	R_1 = 0.0358, wR_2 = 0.0950
Final R indexes [all data]	R_1 = 0.0440, wR_2 = 0.0999
Largest diff. peak/hole / e Å^{-3}	0.74/-0.53

$R_1 = \Sigma||F_o|-|F_c||/\Sigma|F_o|$, $wR_2 = [\Sigma[w(F_o^2-F_c^2)^2]/\Sigma[w(F_o^2)^2]]^{½}$, $w = 1/[\sigma^2(F_o^2) + (aP)^2 + bP]$, where $P = [max(Fo^2,0) + 2Fc^2]/3$

Table S3 Crystal data and structure refinement for **C**$(AuCl)_2$

Empirical formula	$C_{166}H_{204}Au_2Cl_2N_2O_{10}P_2$
Formula weight	2914.07
Temperature/K	200
Crystal system	triclinic
Space group	P-1
a/Å	14.1201(3)
b/Å	14.4758(3)
c/Å	18.9307(3)
α/°	88.005(2)
β/°	85.593(2)
γ/°	86.527(2)
Volume/Å^3	3849.14(13)
Z	1
ρ_{calc}g/cm^3	1.257
μ/mm^{-1}	2.015
F(000)	1516.0
Crystal size/mm^3	0.15 × 0.05 × 0.04
Radiation	MoKα (λ = 0.71073)
2Θ range for data collection/°	3.604 to 51.364
Index ranges	-17 ≤ h ≤ 17, -17 ≤ k ≤ 17, -23 ≤ l ≤ 23
Reflections collected	103242
Independent reflections	14588 [R_{int} = 0.0559, R_{sigma} = 0.0352]
Data/restraints/parameters	14588/627/993
Goodness-of-fit on F^2	1.050
Final R indexes [I>=2σ (I)]	R_1 = 0.0374, wR_2 = 0.0833
Final R indexes [all data]	R_1 = 0.0428, wR_2 = 0.0871
Largest diff. peak/hole / e Å^{-3}	1.01/-0.67

$R_1 = \Sigma||F_o|-|F_c||/\Sigma|F_o|$, $wR_2 = [\Sigma[w(F_o^2-F_c^2)^2]/\Sigma[w(F_o^2)^2]]^{½}$, $w = 1/[\sigma^2(F_o^2) + (aP)^2 + bP]$, where $P = [max(Fo^2,0) + 2Fc^2]/3$

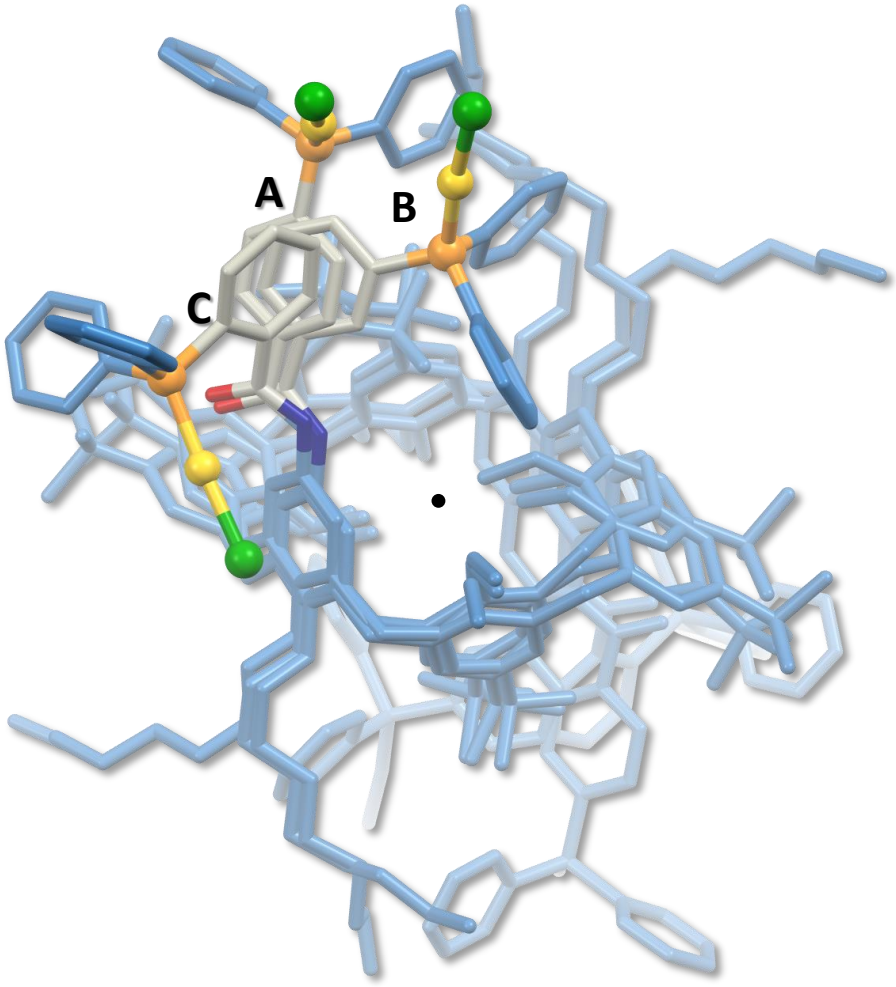

Figure S 4 Overlay between **A-C**$(AuCl)_2$ complexes, showing the phospine orientation in relation to calculated cavity centroid (black dot)

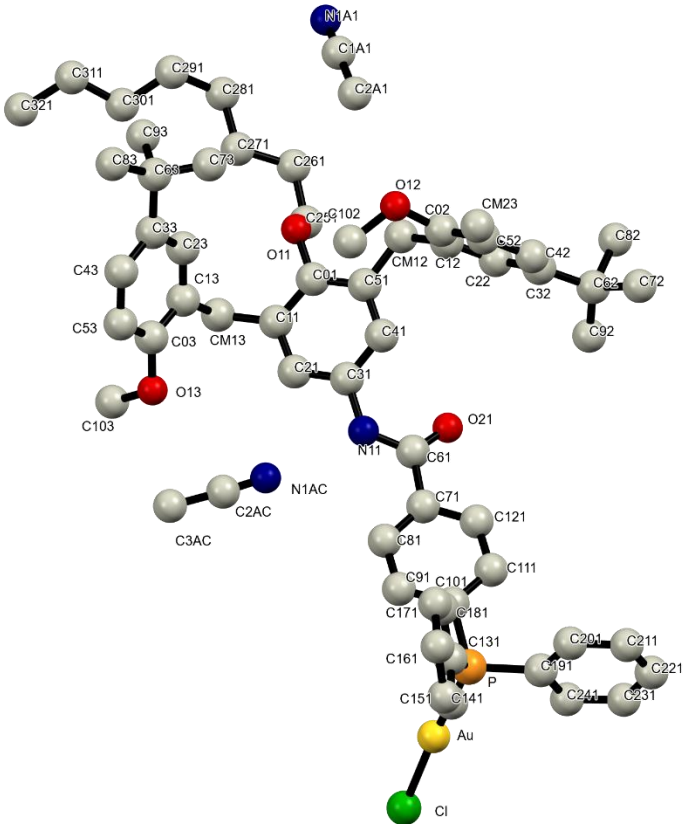

Figure S 5 Ball and stick representation and labelling scheme for **A**$(AuCl)_2$ complex (disorder is omitted for clarity)

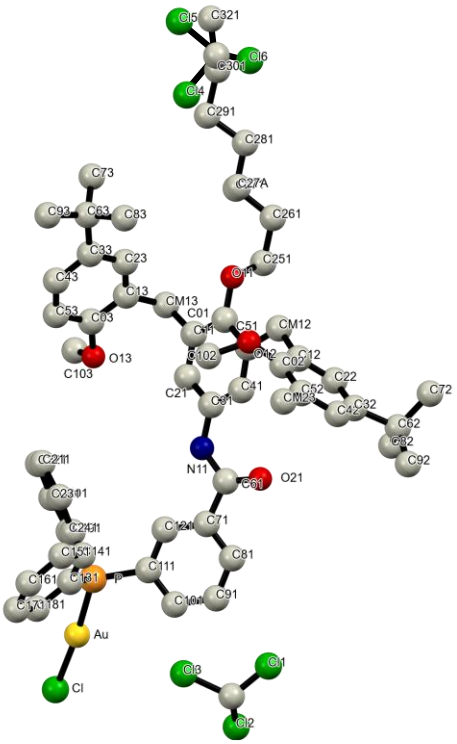

Figure S 6 Ball and stick representation and labelling scheme for **B**$(AuCl)_2$ complex (disorder is omitted for clarity)

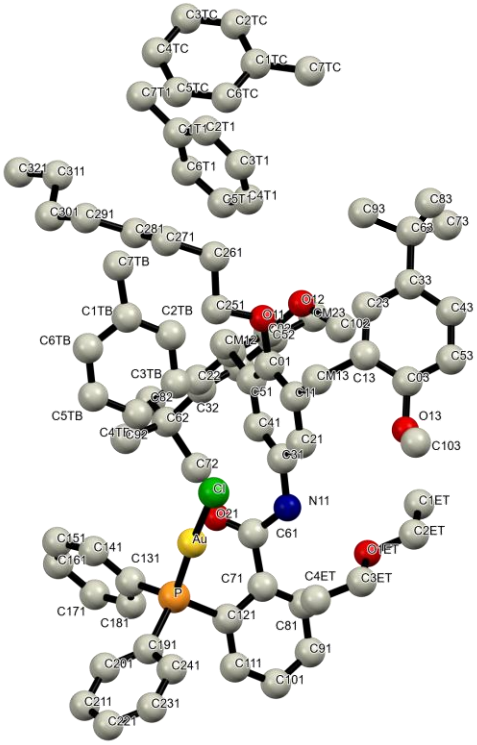

Figure S 7 Ball and stick representation and labelling scheme for **C**$(AuCl)_2$ complex (disorder is omitted for clarity)

	A$(AuCl)_2$	**B**$(AuCl)_2$	**C**$(AuCl)_2$
		Gold Coordination	
Au-P	2.222(2)	2.233(1)	2.2328(9)
Au-P	2.268(2)	2.283(1)	2.285(1)
P-Au-Cl	175.51(7)	175.20(4)	175.28(4)
		CH$\cdots\pi$ intramolecular *interactions*	
C102···C51	3.362(9)	3.554(6)	3.394(5)
C102···C53	3.354(8)	3.433(6)	3.484(6)
C102···C43	3.569(7)	-	3.641(6)

Table S4 Selected geometrical (Å, °) parameters for complexes **A**-**C**$(AuCl)_2$

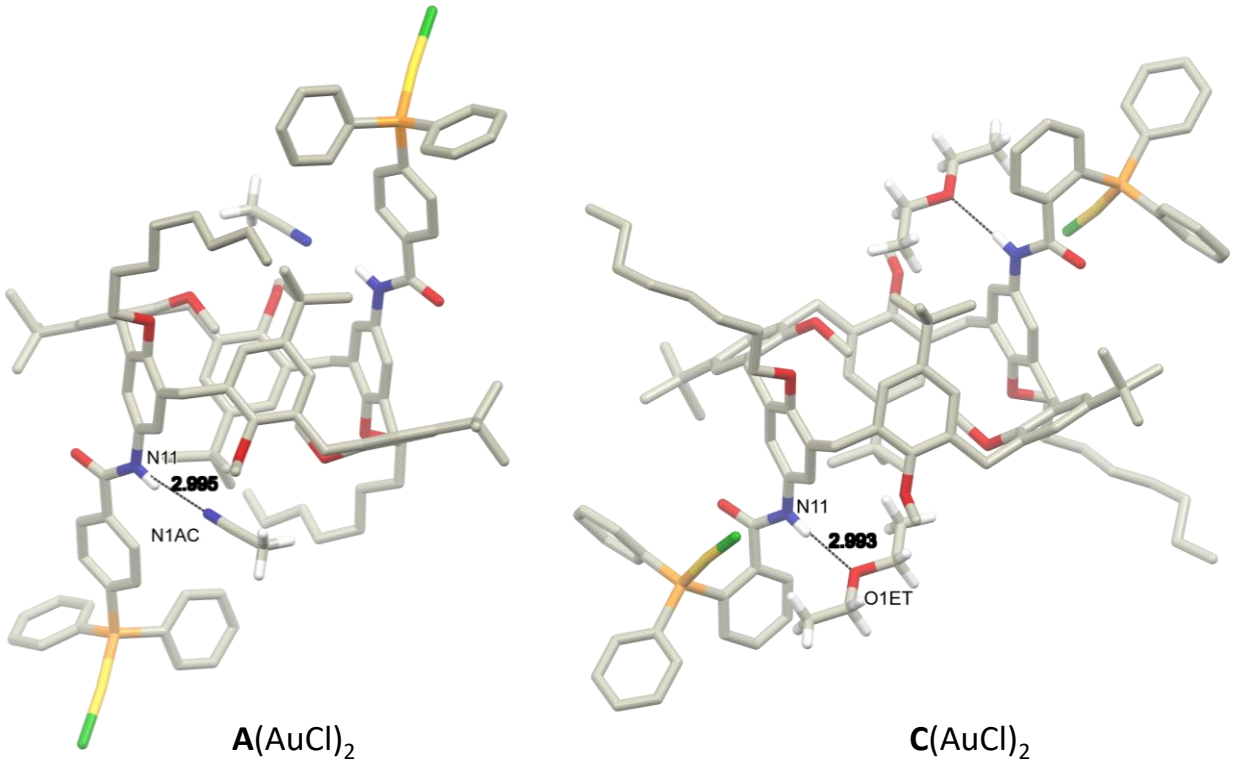

Figure S 8 Hydrogen bond interactions between acetonitrile molecule and **A**$(AuCl)_2$ (on the left); diethyl ether molecule and **C**$(AuCl)_2$ (on the right)

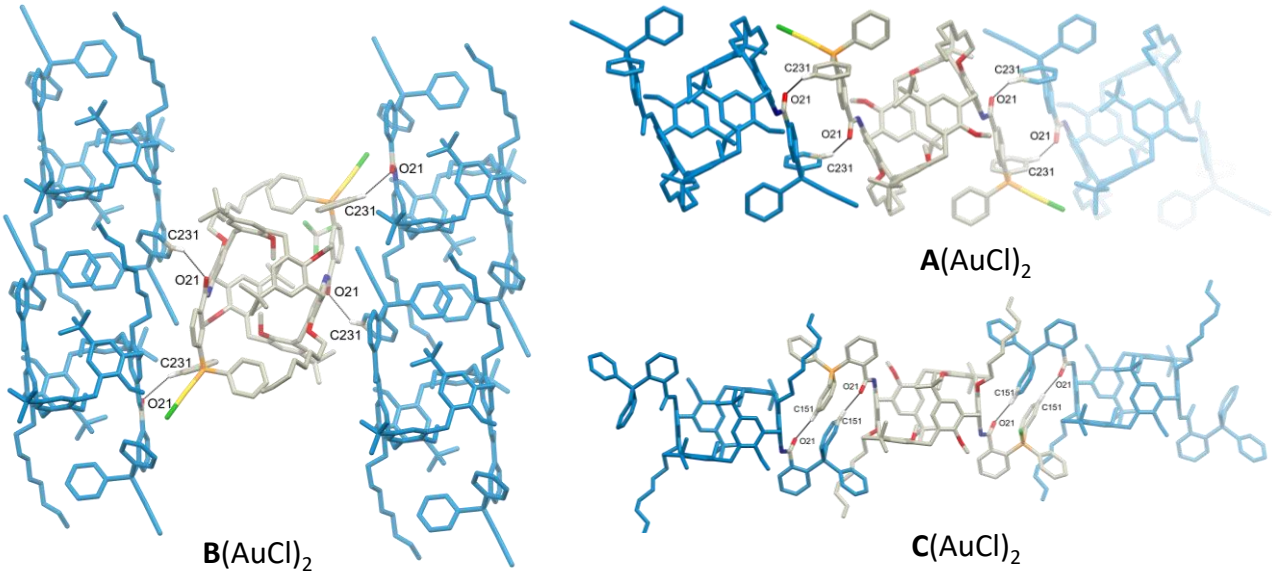

Figure S 9 Packing and intermolecular CH---O weak interactions for **A-C**$(AuCl)_2$

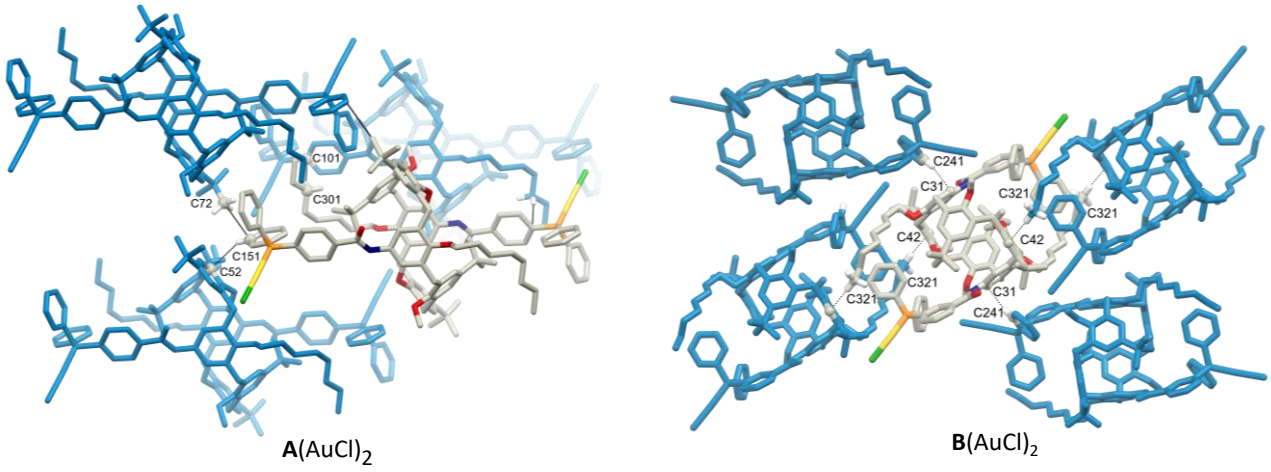

A(AuCl)$_2$ **B**(AuCl)$_2$

Figure S 10 Packing and CH-π weak intermolecular interactions for **A**(AuCl)$_2$ and **B**(AuCl)$_2$

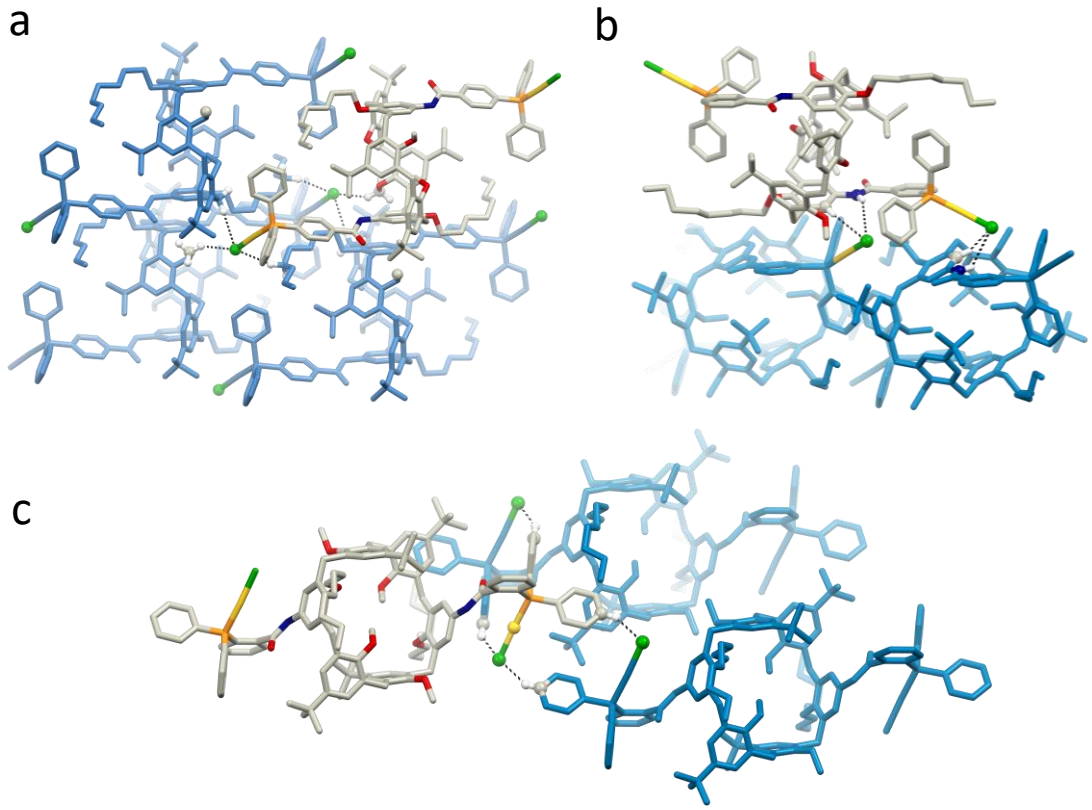

Figure S 11 Weak intermolecular CH---Cl interactions for **A**(AuCl)$_2$ (a), **B**(AuCl)$_2$ (b), **C**(AuCl)$_2$ (c)

Packing Images

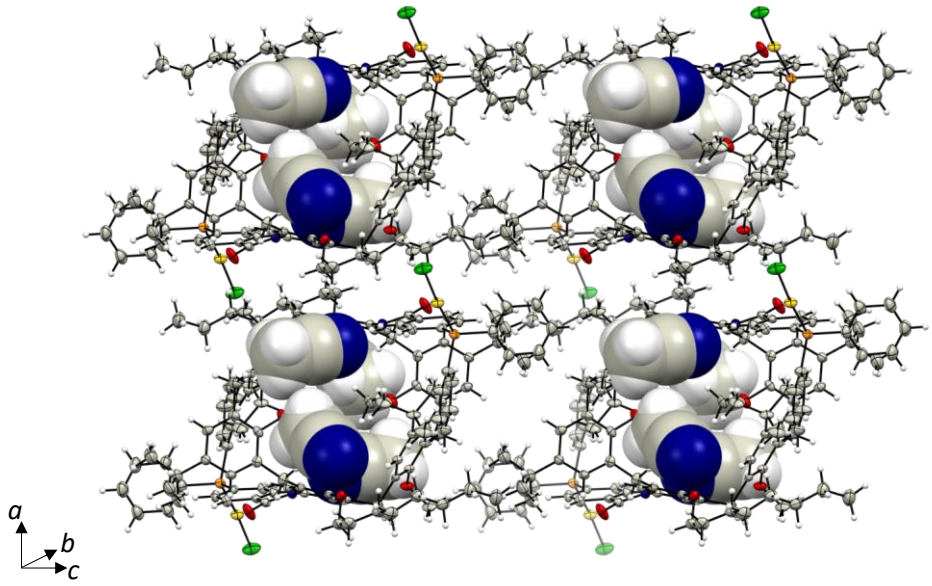

Figure S 12 Packing view along crystallographic axis *b* for **A**$(AuCl)_2$: thermal ellipsoids style for complex molecules, spacefill style for acetonitrile solvent

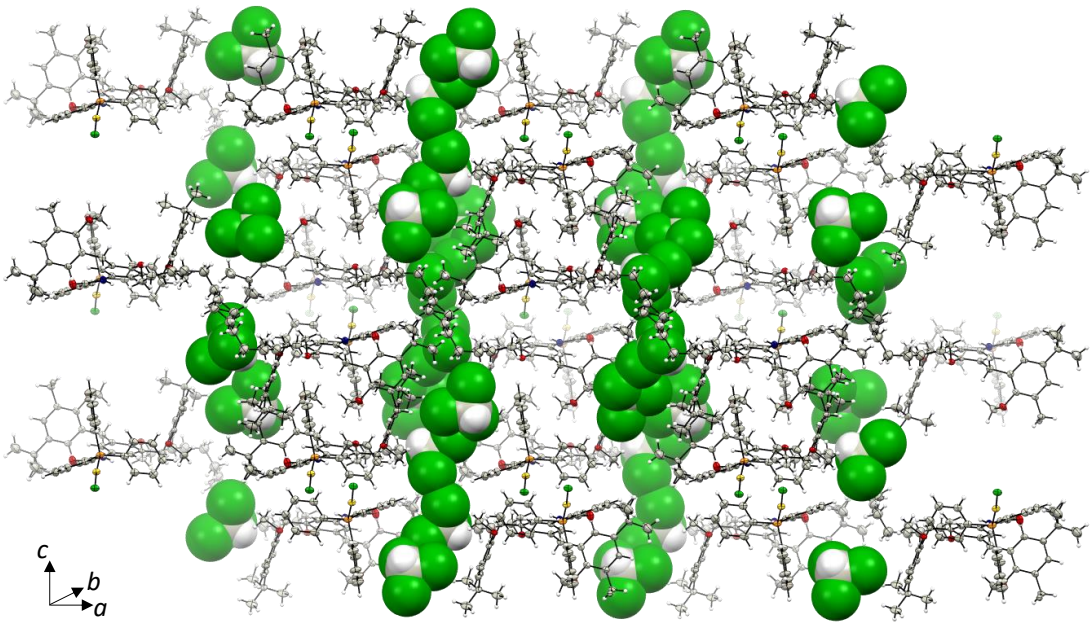

Figure S 13 Packing view along crystallographic axis *b* for **B**$(AuCl)_2$: thermal ellipsoids style for complex molecules, spacefill style for chloroform molecules

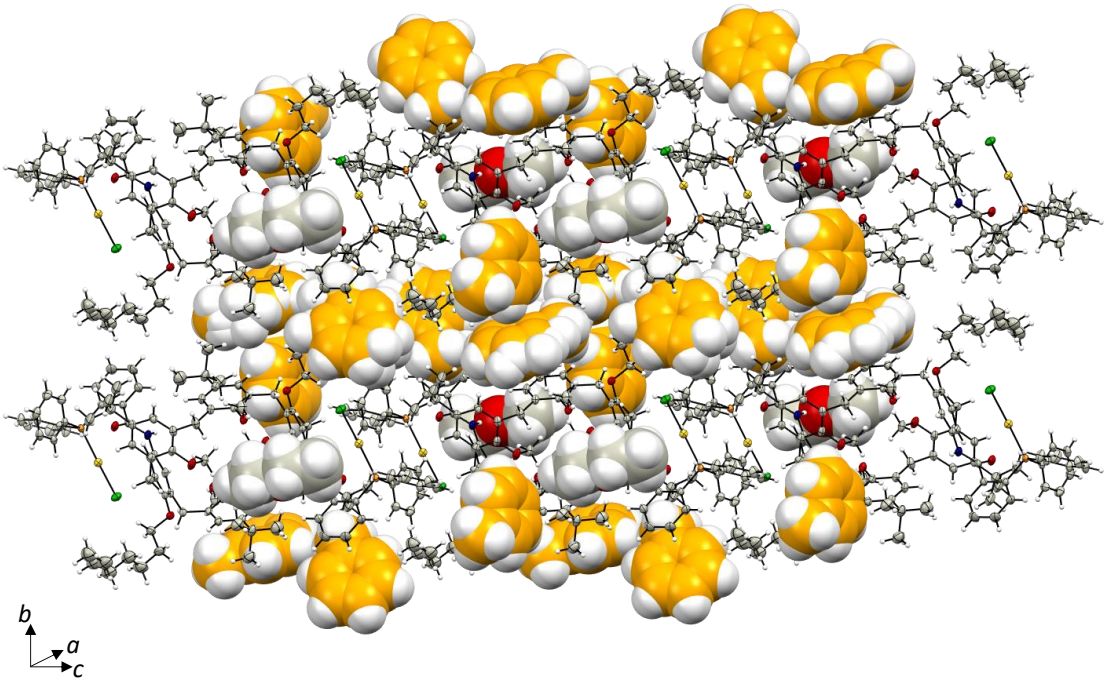

Figure S 14 Packing view along crystallographic axis *a* for **C**$(AuCl)_2$: thermal ellipsoids style for complex molecules, spacefill style for solvent molecules of crystallization (yellow carbon for toluene, grey carbon for diethyl ether)

Electron density maps

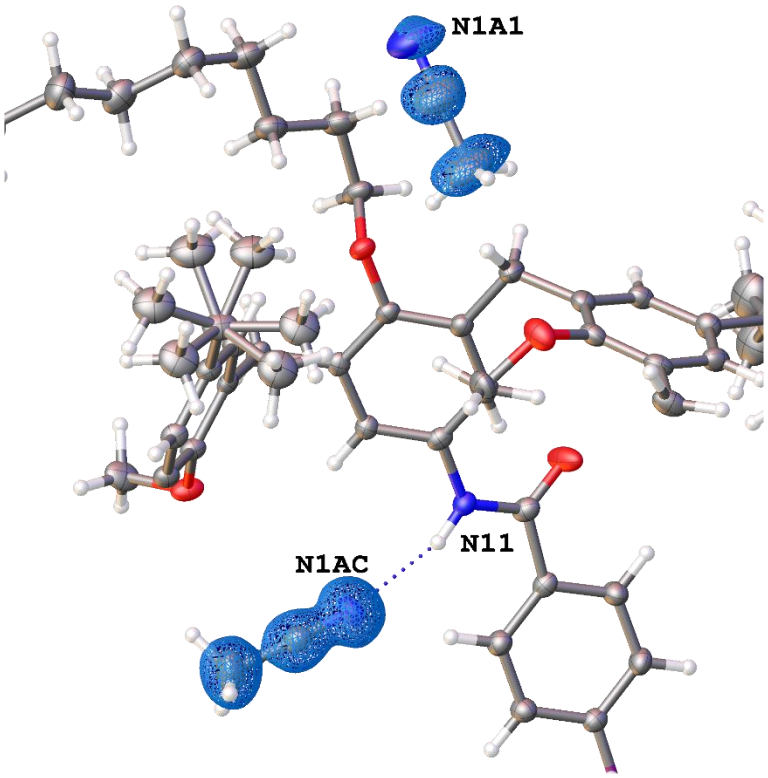

Figure S 15 Overlay between acetonitrile molecules and residual electron density map (diff., 1.2 e^- level) for **A**$(AuCl)_2$

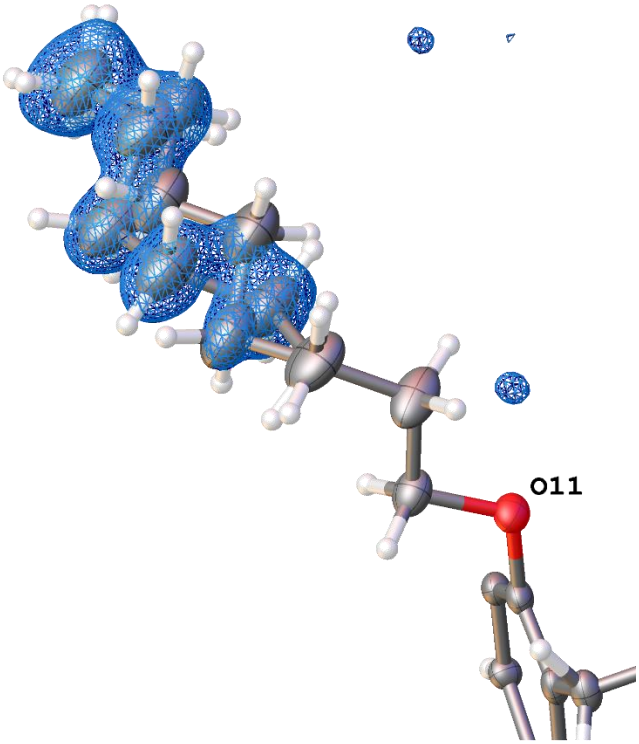

Figure S 16 Overlay between residual electron density map (diff, 0.8 e^- level) and disordered octyl tail for **B**$(AuCl)_2$

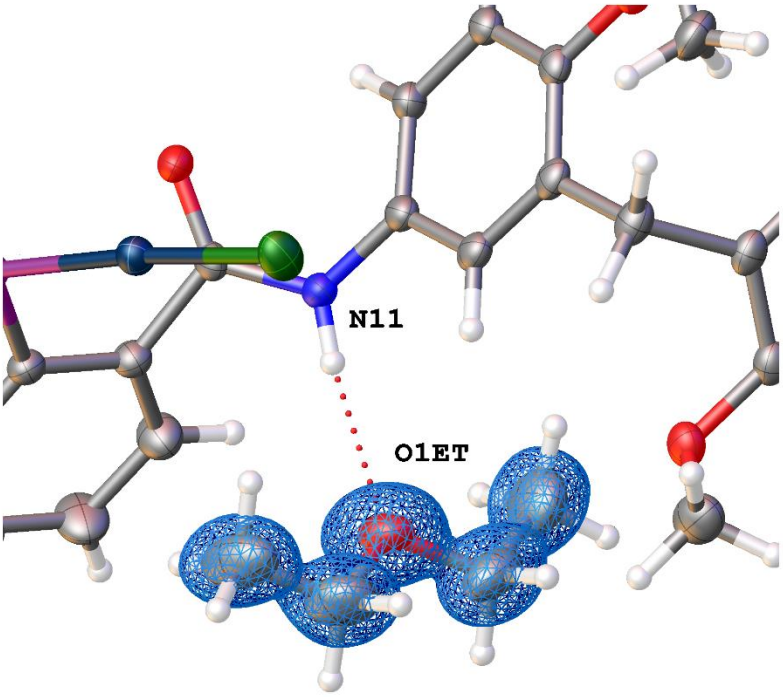

Figure S 17 Overlay between H-bonded diethyl ether molecule and residual electron density map plot (difference, 1.2 electron level) for **C**$(AuCl)_2$

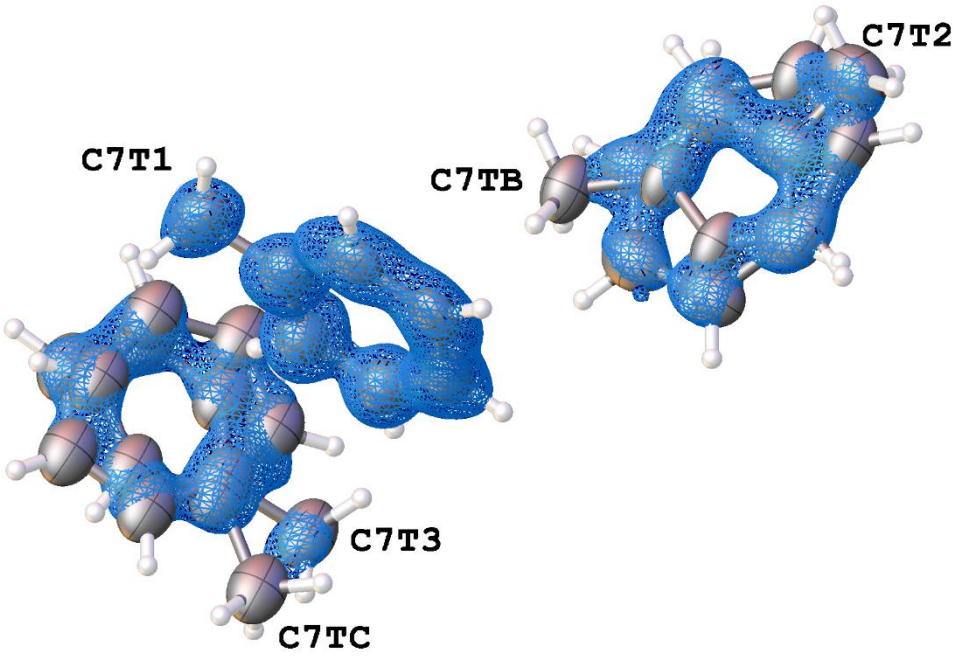

Figure S 18 Overlay between modelled toluene molecules of crystallization and residual electron density map (difference, 1.2 electron level for **C**$(AuCl)_2$

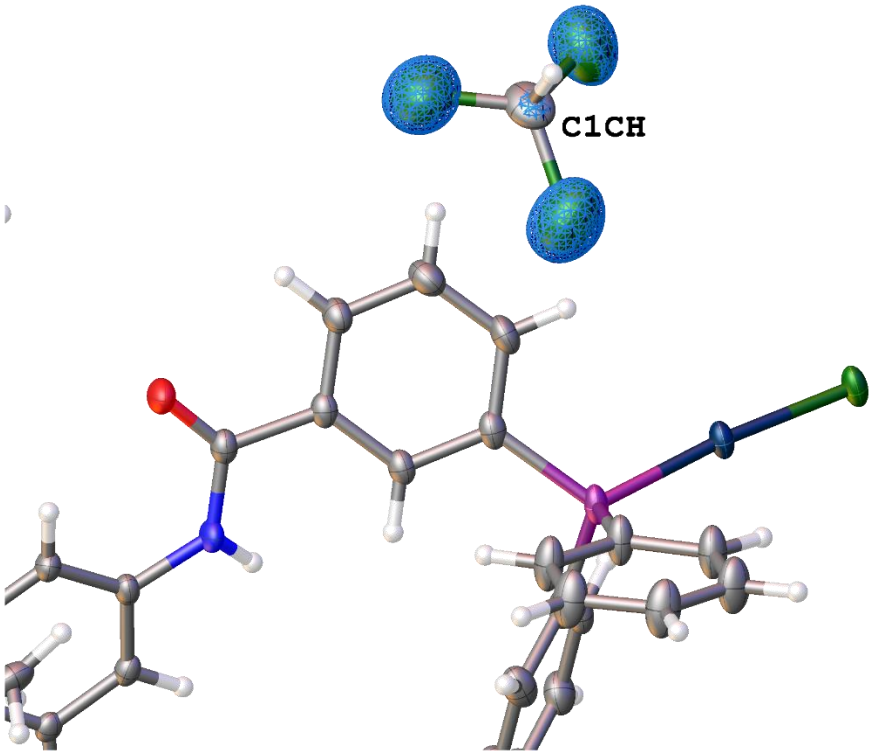

Figure S 19 Overlay between residual electron density map (diff, 2.0 electron level) and modelled chloroform molecule solvent of crystallization for **B**$(AuCl)_2$

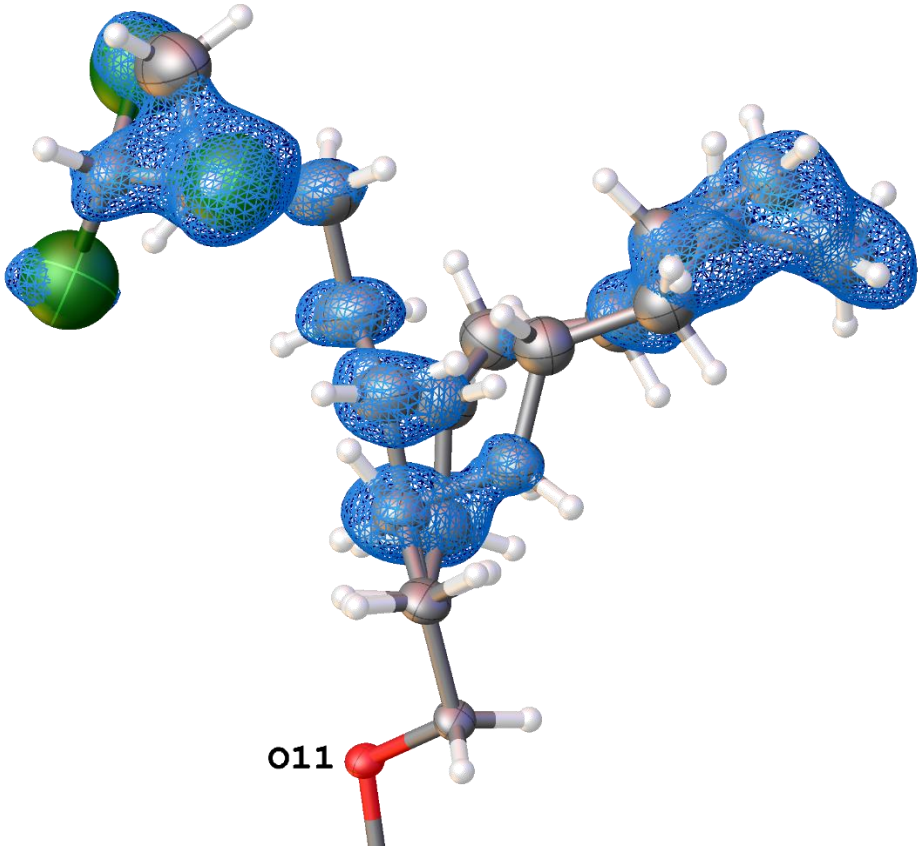

Figure S 20 Alternative orientations for octyl chain and chloroform solvent overlaid with electron residual map (diff, 0.8 electron level) for **B**$(AuCl)_2$

- **Variable Temperature NMR Analysis**

Stack plot of the ^{1}H-NMR (1,1,2,2-tetrachloroethane-d_2, 400 MHz) spectra of **A**$(AuCl)_2$ at different temperatures.

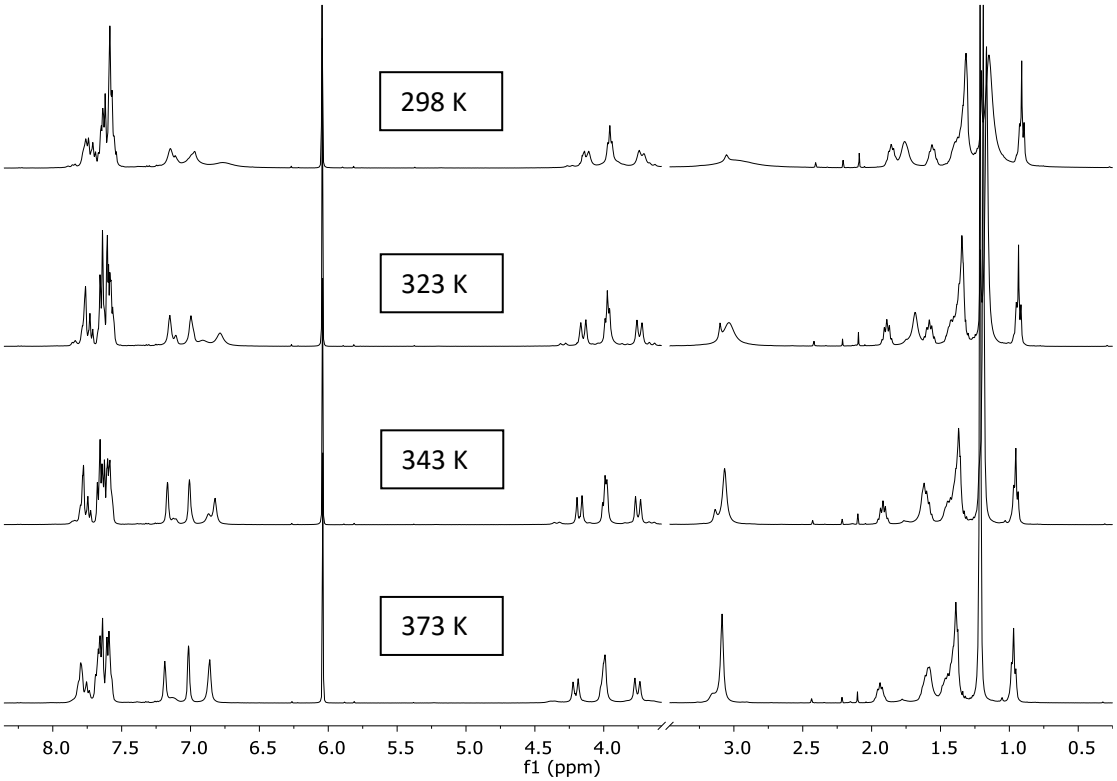

Stack plot of the ^{1}H-NMR ($CDCl_3$, 400 MHz) spectra of **A**$(AuCl)_2$ at different temperatures.

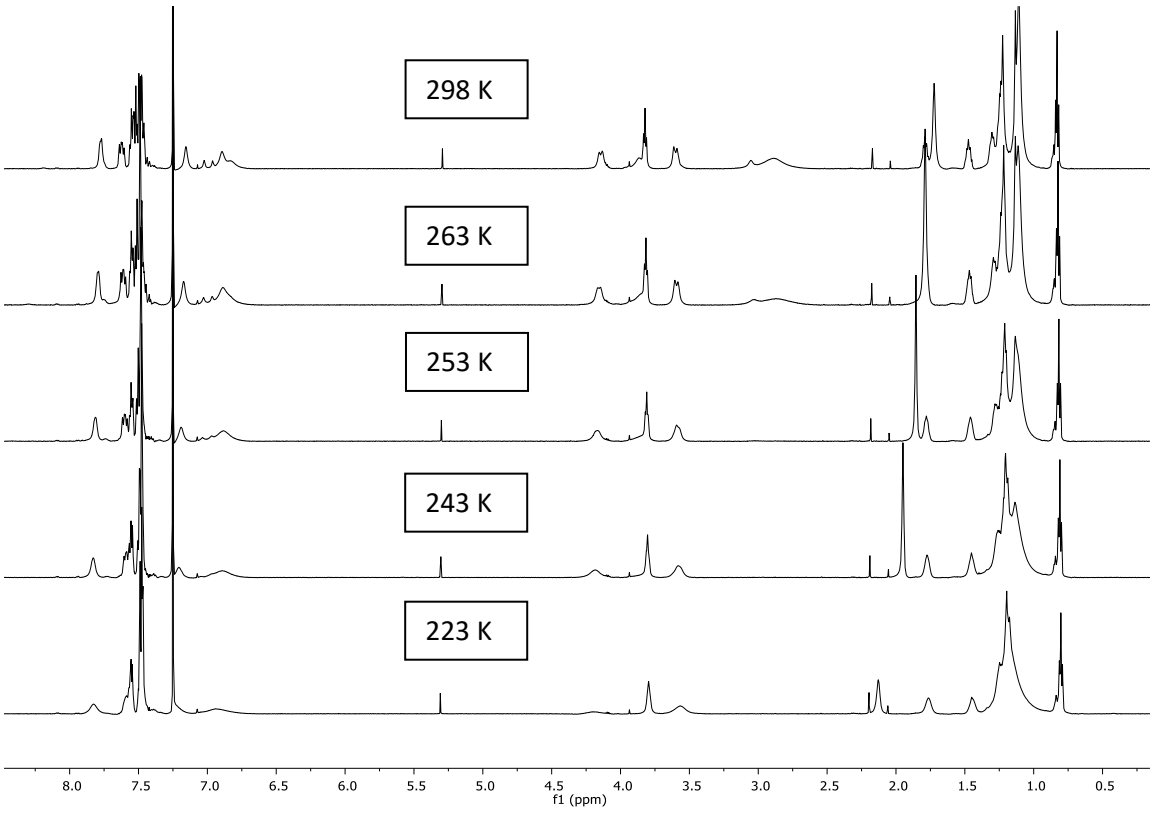

- **Synthesis and Characterisation of Novel Enynes 1**

Method A

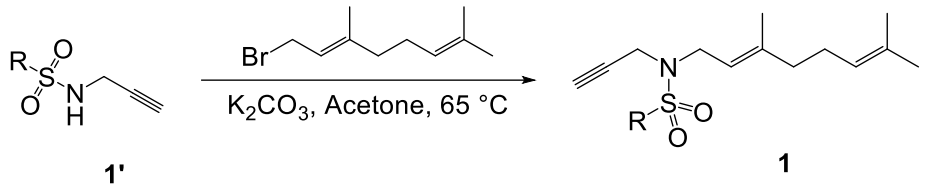

In a Schlenk flask, geranyl bromide (1.2 equiv.) was added dropwise to a solution of the corresponding *N*-substituted-propargylsulfonamide derivative (1.0 equiv) and K_2CO_3 (1.5 equiv) in acetone (10 ml). Subsequently, the mixture was placed in a pre-heated oil bath at 50 °C and stirred overnight. After completion, the reaction mixture was cooled down to room temperature and HCl 10 % (15 ml) was added. The mixture was extracted with EtOAc (3 x 15 ml), the organic layers separated and dried over Na_2SO_4. The combined fractions were concentrated under reduced pressure and the crude purified by column chromatography on silica gel.

Method B

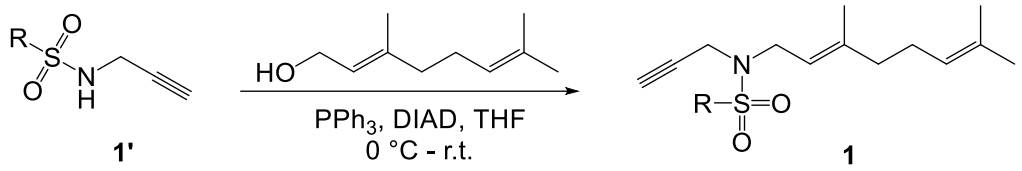

In an oven-dried two-necked round-bottomed flask, geraniol (1.2 equiv) was added to a 1.0 M solution in THF of the corresponding *N*-substituted-propargylsulfonamide derivative (1.0 equiv) and PPh_3 (1.2 equiv) under N_2 atmosphere. Subsequently, the mixture was placed at 0°C and DIAD (1.2 equiv) was carefully added dropwise over 10 min. The mixture was stirred until complete conversion (2-8 hs). Subsequently, a solution of HCl 10 % (10 ml) was added, the mixture extracted with EtOAc (3 x 15 ml), the organic layers separated and dried over Na_2SO_4. The combined fractions were concentrated under reduced pressure and the crude purified by column chromatography on silica gel.

(*E*)-*N*-(3,7-dimethylocta-2,6-dien-1-yl)-4-methoxy-*N*-(prop-2-yn-1-yl)benzenesulfonamide (1c)

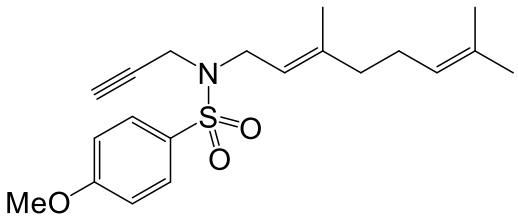

Representative procedure **A** was followed using 4-Methoxy-*N*-(prop-2-yn-1-yl)benzenesulfonamide (270 mg, 1.2 mmol). Purification by column chromatography on silica gel (*n*-hexanes/EtOAc 80:20) yielded **1c** (425 mg, 98 %) as a yellow oil. **^{1}H NMR** (400 MHz, $CDCl_3$) δ = 7.80 (d, *J* = 8.9 Hz, 2H), 6.98 (d, *J* = 8.9 Hz, 2H), 5.11 (m, 1H), 5.05 (m, 1H), 4.08 (d, *J* = 2.4 Hz, 2H), 3.88 (s, 3H), 3.84 (d, *J* = 7.4 Hz, 2H), 2.13 – 2.02 (m, 4H), 2.01 (t, *J* = 2.6 Hz, 1H), 1.69 (s, 3H), 1.68 (s, 3H), 1.60 (s, 3H). **^{13}C NMR** (101 MHz, $CDCl_3$) δ = 162.9 (C_q), 142.5 (C_q), 131.9 (C_q), 130.8 (C_q), 129.9 (CH), 123.7 (CH), 117.83 (CH), 113.9 (CH), 76. 8 (CH), 73.4 (C_q), 55.6 (CH_3), 43.8 (CH_2), 39.6 (CH_2), 35.2 (CH_2), 26.2 (CH_2), 25.7 (CH_3), 17.7 (CH_3), 16.2 (CH_3). **ESI-MS**: *m/z* $[M + Na]^+$ calcd for $C_{20}H_{27}NNaO_3S$: 384.16; found: 384.19.

(*E*)-*N*-(3,7-dimethylocta-2,6-dien-1-yl)-2,4,6-trimethyl-*N*-(prop-2-yn-1-yl)benzenesulfonamide (1d)

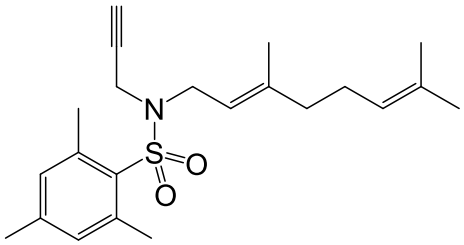

Representative procedure **B** was followed using 2,4,6-Trimethyl-*N*-(prop-2-yn-1-yl)benzenesulfonamide (319 mg, 1.3 mmol). Purification by column chromatography on silica gel (*n*-hexanes/EtOAc 80:20) yielded **1d** (473 mg, 94 %) as a pale-yellow oil. **^{1}H NMR** (400 MHz, $CDCl_3$) δ = 6.97 (s, 2H), 5.12 – 5.00 (m, 2H), 3.99 (d, *J* = 2.4 Hz, 2H), 3.84 (d, *J* = 7.2 Hz, 2H), 2.63 (s, 6H), 2.32 (s, 3H), 2.25 (t, *J* = 2.4 Hz, 1H), 2.12 – 2.00 (m, 4H), 1.69 (s, 3H), 1.65 (s, 3H), 1.61 (s, 3H). **^{13}C NMR** (101 MHz, $CDCl_3$) δ = 142.6 (C_q), 142.4 (C_q), 140.5 (C_q), 131.9 (CH), 123.8 (CH), 117.9 (CH), 77.3 (CH), 72.7 (C_q), 43.0 (CH_2), 39.7 (CH_2), 33.9 (CH_2), 26.2 (CH_2), 25.7 (CH_3), 22.8 (CH_3), 20.7 (CH_3), 17.7 (CH_3), 16.0 (CH_3). **ESI-MS**: *m/z* $[M + Na]^+$ calcd for $C_{22}H_{31}NNaO_2S$: 396.20; found: 396.16.

(E)-4-Chloro-N-(3,7-dimethylocta-2,6-dien-1-yl)-N-(prop-2-yn-1-yl)benzenesulfonamide (1e)

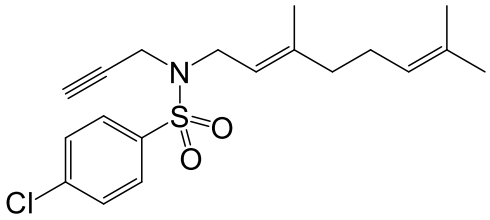

Representative procedure **B** was followed using 4-Chloro-*N*-(prop-2-yn-1-yl)benzenesulfonamide (200 mg, 1.3 mmol). Purification by column chromatography on silica gel (*n*-hexanes/EtOAc 80:20) yielded **1e** (462 mg, 97 %) as a colourless oil. **^{1}H NMR** (400 MHz, $CDCl_3$) δ = 7.82 (d, *J* = 8.6 Hz, 2H), 7.49 (d, *J* = 8.6 Hz, 2H), 5.16 – 5.09 (m, 1H), 5.09 – 5.01 (m, 1H), 4.10 (d, *J* = 2.6 Hz, 2H), 3.85 (d, *J* = 7.2 Hz, 2H), 2.14 – 2.04 (m, 4H), 2.01 (t, *J* = 2.3 Hz, 1H), 1.72 – 1.67 (m, 6H), 1.61 (s, 3H). **^{13}C NMR** (101 MHz, $CDCl_3$) δ = 143.0 (C_q), 139. (C_q), 137.7 (C_q), 132.0 (C_q), 129.3 (CH), 129.1 (CH), 123.7 (CH), 117.4 (CH), 77.3 (CH), 73.7 (C_q), 43.9 (CH_2), 39.6 (CH_2), 35.3 (CH_2), 26.1 (CH_2), 25.7 (CH_3), 17.7 (CH_3), 16.2 (CH_3). **ESI-MS**: *m/z* $[M + Na]^+$ calcd for $C_{19}H_{24}ClNNaO_2S$: 388.11; found: 388.11.

(*E*)-*N*-(3,7-dimethylocta-2,6-dien-1-yl)-4-iodo-*N*-(prop-2-yn-1-yl)benzenesulfonamide (1f)

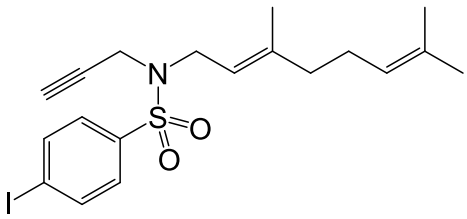

Representative procedure **A** was followed using 4-Iodo-*N*-(prop-2-yn-1-yl)benzenesulfonamide (320 mg, 1.0 mmol). Purification by column chromatography on silica gel (*n*-hexanes/EtOAc 80:20) yielded **1f** (375 mg, 82%) as a white solid. **M. p.** = 47 – 48 °C. **^{1}H NMR** (400 MHz, $CDCl_3$) δ = 7.88 (d, *J* = 8.7 Hz, 2H), 7.69 (d, *J* = 8.7 Hz, 2H), 5.11 (m, 1H), 5.05 (m, 1H), 4.09 (d, *J* = 2.6 Hz, 2H), 3.85 (d, *J* = 7.3 Hz, 2H), 2.14 – 2.03 (m, 4H), 2.02 (t, *J* = 2.4 Hz, 1H), 1.69 (s, 3H), 1.68 (s, 3H), 1.61 (s, 3H). **^{13}C NMR** (101 MHz, $CDCl_3$) δ = 143.0 (C_q), 138.9 (C_q), 138.0 (CH), 132.0 (C_q), 129.2 (CH), 123.7 (CH), 117.4 (CH), 100.0 (C_q), 76.9 (CH), 73.7 (C_q), 43.9 (CH_2), 39.6 (CH_2), 35.2 (CH_2), 26.1 (CH_2), 25.7 (CH_3), 17.7 (CH_3), 16.2 (CH_3). **ESI-MS**: *m/z* $[M + Na]^+$ calcd for $C_{19}H_{24}INNaO_2S$: 480.05; found: 480.02.

(*E*)-2-Bromo-*N*-(3,7-dimethylocta-2,6-dien-1-yl)-*N*-(prop-2-yn-1-yl)benzenesulfonamide (1g)

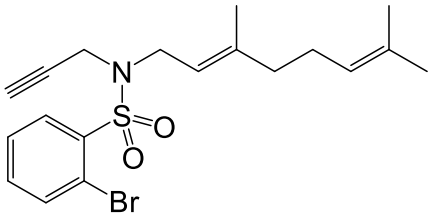

Representative procedure **B** was followed using 2-Bromo-N-(prop-2-yn-1-yl)benzenesulfonamide (271 mg, 1.0 mmol). Purification by column chromatography on silica gel (*n*-hexanes/EtOAc 80:20) yielded **1g** (350 mg, 86 %) as a colourless oil. **^{1}H NMR** (400 MHz, $CDCl_3$) δ = 8.17 (dd, *J* = 7.7, 1.9 Hz, 1H), 7.76 (dd, *J* = 7.7, 1.4 Hz, 1H), 7.46 (td, *J* = 7.5, 1.4 Hz, 1H), 7.40 (td, *J* = 7.7, 1.9 Hz, 1H), 5.13 – 5.00 (m, 2H), 4.15 (d, *J* = 2.6 Hz, 2H), 4.02 (d, *J* = 7.2 Hz, 2H), 2.19 (t, *J* = 2.4 Hz, 1H), 2.12 – 1.99 (m, 4H), 1.69 (s, 3H), 1.67 (s, 3H), 1.61 (s, 3H). **^{13}C NMR** (101 MHz, $CDCl_3$) δ = 142.6 (C_q), 139.2 (C_q), 135.6 (CH), 133.5 (CH), 132.2 (CH), 131.9 (C_q), 127.5 (CH), 123.7 (CH), 120.7 (C_q), 117.8 (CH), 77.4 (CH), 72.9 (C_q), 44.2 (CH_2), 39.6 (CH_2), 35.4 (CH_2), 26.2 (CH_2), 25.7 (CH_3), 17.7 (CH_3), 16.0 (CH_3). **ESI-MS**: *m/z* $[M + Na]^+$ calcd for $C_{19}H_{24}BrNNaO_2S$: 434.06; found: 434.06.

(*E*)-*N*-(3,7-dimethylocta-2,6-dien-1-yl)-4-nitro-*N*-(prop-2-yn-1-yl)benzenesulfonamide (1h)

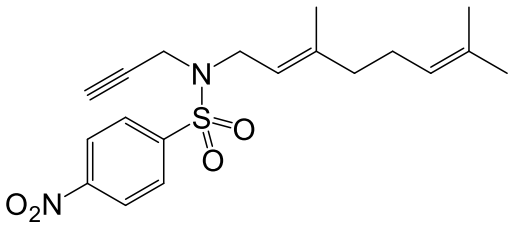

Representative procedure **B** was followed using 4-Nitro-*N*-(prop-2-yn-1-yl)benzenesulfonamide (277 mg, 1.2 mmol). Purification by column chromatography on silica gel (*n*-hexanes/EtOAc 80:20) yielded **1h** (396 mg, 91 %) as a waxy pale-yellow solid. **^{1}H NMR** (400 MHz, $CDCl_3$) δ = 8.37 (d, *J* = 8.8 Hz, 2H), 8.07, (d, *J* = 8.8 Hz, 2H), 5.18 – 5.09 (m, 1H), 5.09 – 5.00 (m, 1H), 4.14 (m, 2H), 3.89 (d, *J* = 7.4 Hz, 2H), 2.17 – 2.04 (m, 4H), 2.01 (t, *J* = 2.6 Hz, 1H), 1.69 (s, 6H), 1.61 (s, 3H). **^{13}C NMR** (101 MHz, $CDCl_3$) δ = 150.1 (C_q), 145.0 (C_q), 143.6 (C_q), 132.1 (C_q), 129.0 (CH), 124.0 (CH), 123.6 (CH), 117.0 (CH), 77.0 (CH), 74.0 (C_q), 44.1 (CH_2), 39.6 (CH_2), 35.3 (CH_2), 26.1 (CH_2), 25.7 (CH_3), 17.7 (CH_3), 16.4 (CH_3). **ESI-MS**: *m/z* $[M + Na]^+$ calcd for $C_{19}H_{24}N_2NaO_4S$: 399.14; found: 399.24.

(*E*)-*N*-(3,7-dimethylocta-2,6-dien-1-yl)-*N*-(prop-2-yn-1-yl)naphthalene-2-sulfonamide (1i)

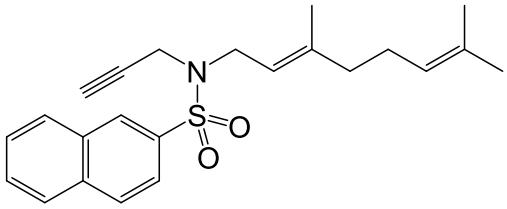

Representative procedure **B** was followed using *N*-(prop-2-yn-1-yl)naphthalene-2-sulfonamide (383 mg, 1.6 mmol). Purification by column chromatography on silica gel (*n*-hexanes/EtOAc 80:20) yielded **1i** (465 mg, 78 %) as a colourless oil. **^{1}H NMR** (400 MHz, $CDCl_3$) δ = 8.46 (s, 1H), 8.02 – 7.91 (m, 3H), 7.87 (dd, *J* = 8.7, 2.0 Hz, 1H), 7.65 (m, 2H), 5.13 (m, 1H), 5.04 (m, 1H), 4.16 (d, *J* = 2.4 Hz, 2H), 3.92 (d, *J* = 7.2 Hz, 2H), 2.14 – 2.00 (m, 4H), 1.90 (t, *J* = 2.4 Hz, 1H), 1.69 (s, 3H), 1.67 (s, 3H), 1.59 (s, 3H). **^{13}C NMR** (101 MHz, $CDCl_3$) δ = 142.7 (C_q), 136.1 (C_q), 134.9 (C_q), 132.2 (C_q), 131.9 (C_q), 129.3 (CH), 129.2 (CH), 128.9 (CH), 128.7 (CH), 127.9 (CH), 127.4 (CH), 123.7 (CH), 123.2 (CH), 117.7 (CH), 76.7 (CH), 73.4 (C_q), 44.0 (CH_2), 39.6 (CH_2), 35.4 (CH_2), 26.2 (CH_2), 25.7 (CH_3), 17.7 (CH_3), 16.1 (CH_3). **ESI-MS**: *m/z* for $[M + K]^+$ calcd for $C_{23}H_{27}KNO_2S$: 420.14; found: 420.10.

(E)-N-(3,7-dimethylocta-2,6-dien-1-yl)-N-(prop-2-yn-1-yl)ferrocene-sulfonamide (1j)

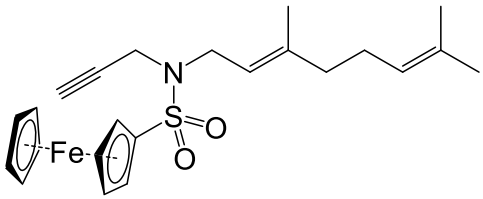

Representative procedure **A** was followed using *N*-(prop-2-yn-1-yl)ferrocene-sulfonamide (303 mg, 1.0 mmol). Purification by column chromatography on silica gel (*n*-hexanes/EtOAc 80:20) yielded **1j** (381 mg, 87%) as a brown solid. **M. p.** = 83 – 84 °C. **^{1}H NMR** (400 MHz, $CDCl_3$) δ = 5.13 – 5.02 (m, 2H), 4.69 (s, 2H), 4.43 (s, 5H), 4.39 (s, 2H), 3.96 (d, *J* = 2.5 Hz, 2H), 3.75 (d, *J* = 7.2 Hz, 2H), 2.12 – 2.00 (m, 5H), 1.69 (s, 3H), 1.67 (s, 3H), 1.60 (s, 3H). **^{13}C NMR** (101 MHz, $CDCl_3$) δ = 142.1 (C_q), 131.8 (C_q), 123.8 (CH), 117.9 (CH), 86.0 (C_q), 77.2 (CH), 73.5 (C_q), 70.8 (CH), 70.4 (CH), 69.4 (CH), 43.7 (CH_2), 39.6 (CH_2), 35.3 (CH_2), 26.2 (CH_2), 25.7 (CH_3), 17.7 (CH_3), 16.2 (CH_3). **ESI-MS**: *m/z* $[M + Na]^+$ calcd for $C_{23}H_{29}FeNNaO_2S$: 462.12; found: 462.06.

- **Copies of NMR Spectra for Compounds 1 and 2**

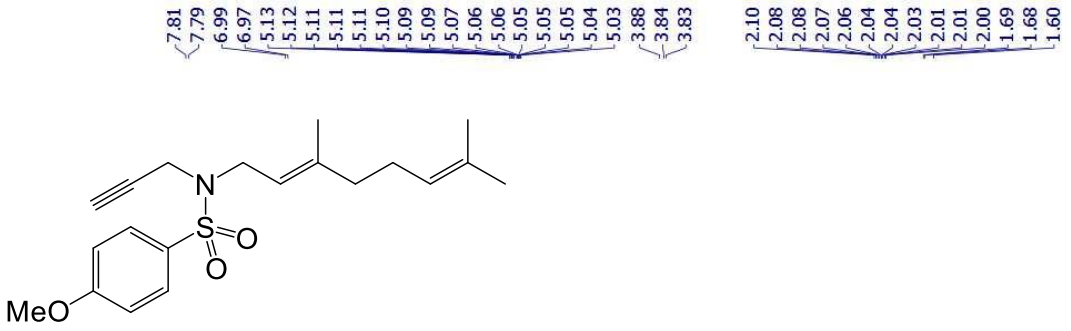

1c (400 MHz, $CDCl_3$)

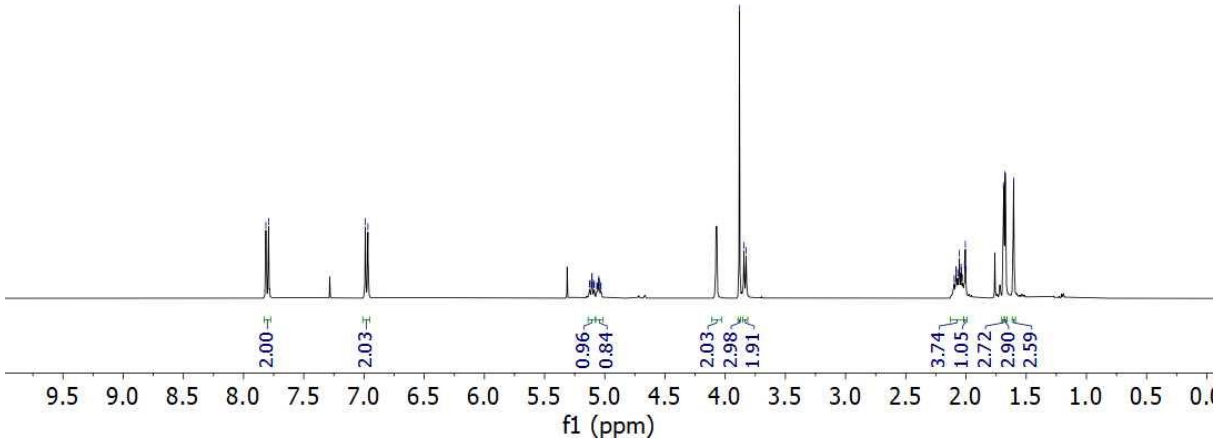

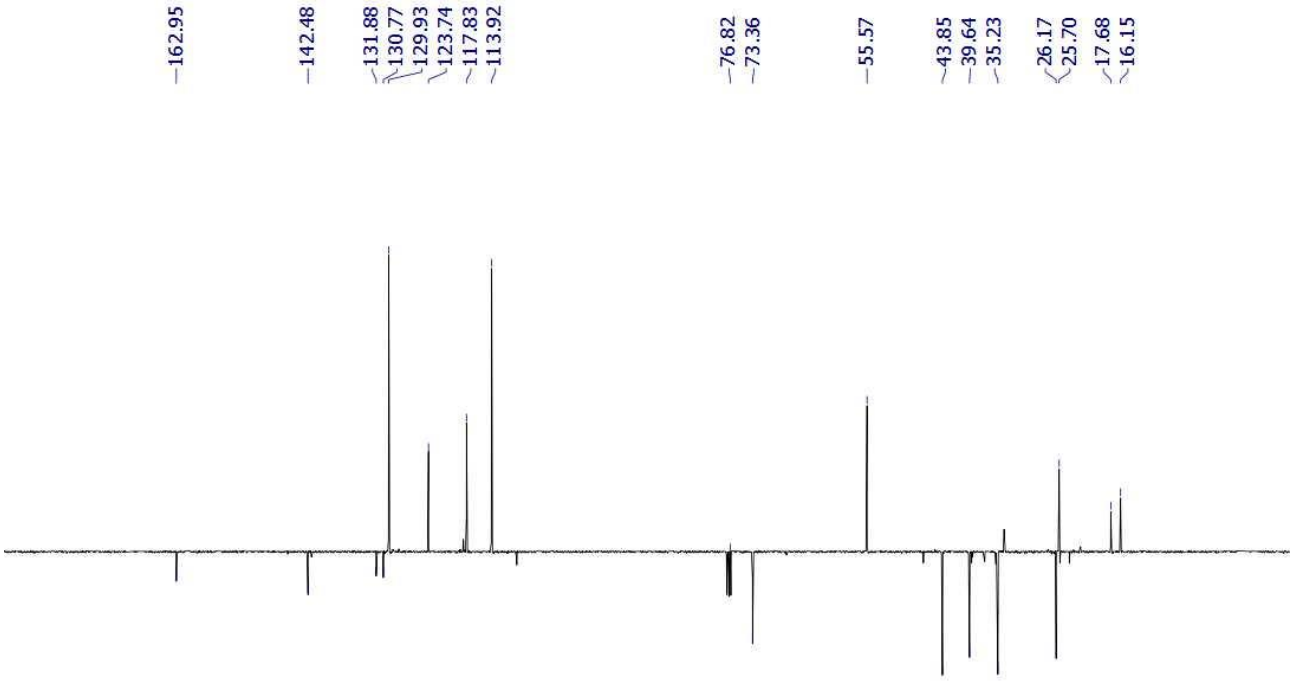

1c (101 MHz, $CDCl_3$)

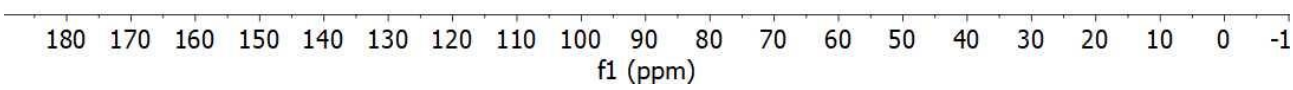

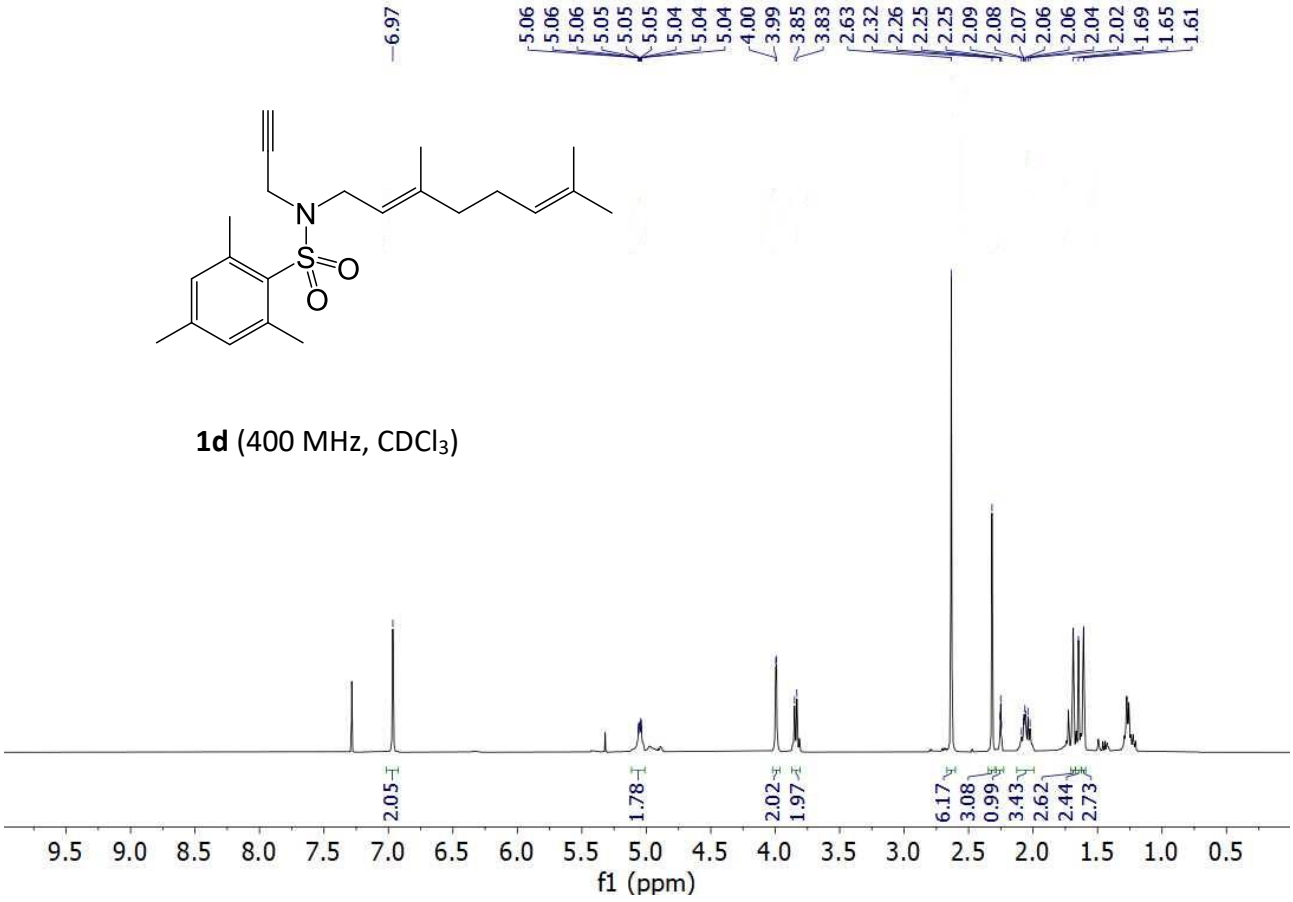

1d (400 MHz, $CDCl_3$)

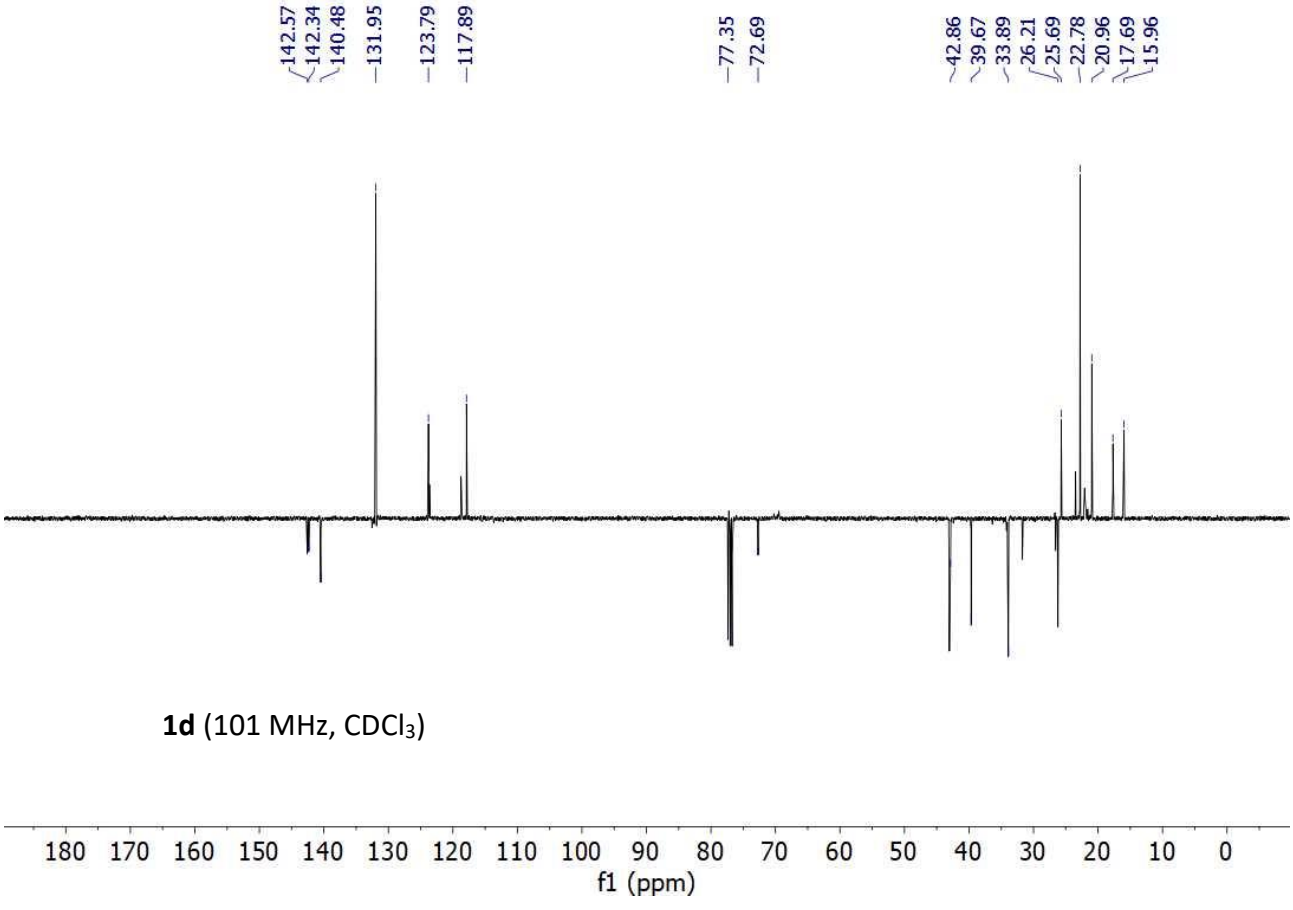

1d (101 MHz, $CDCl_3$)

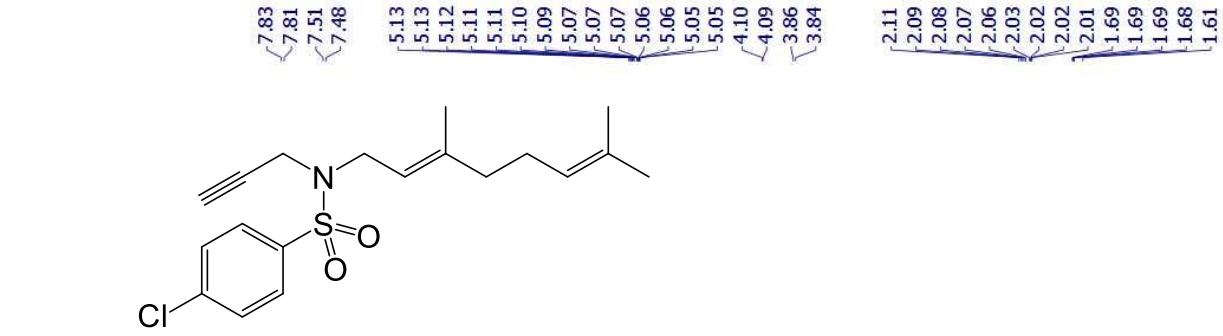

1e (400 MHz, $CDCl_3$)

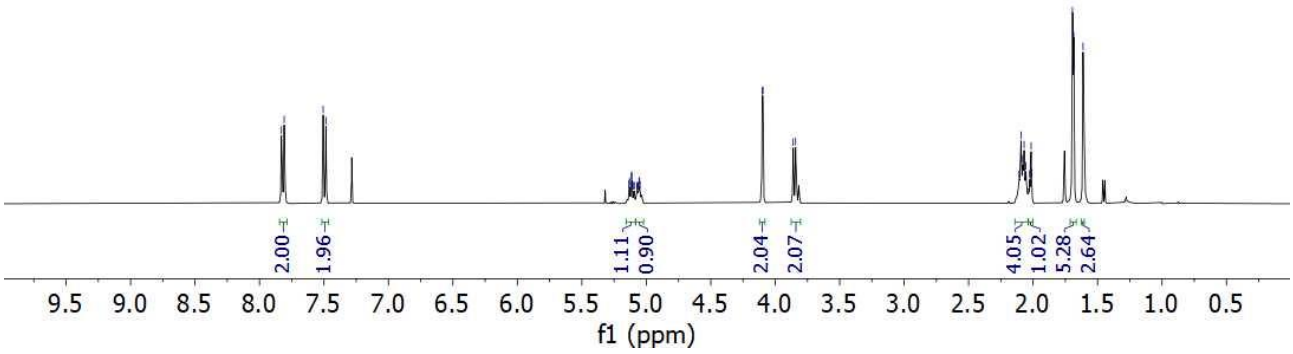

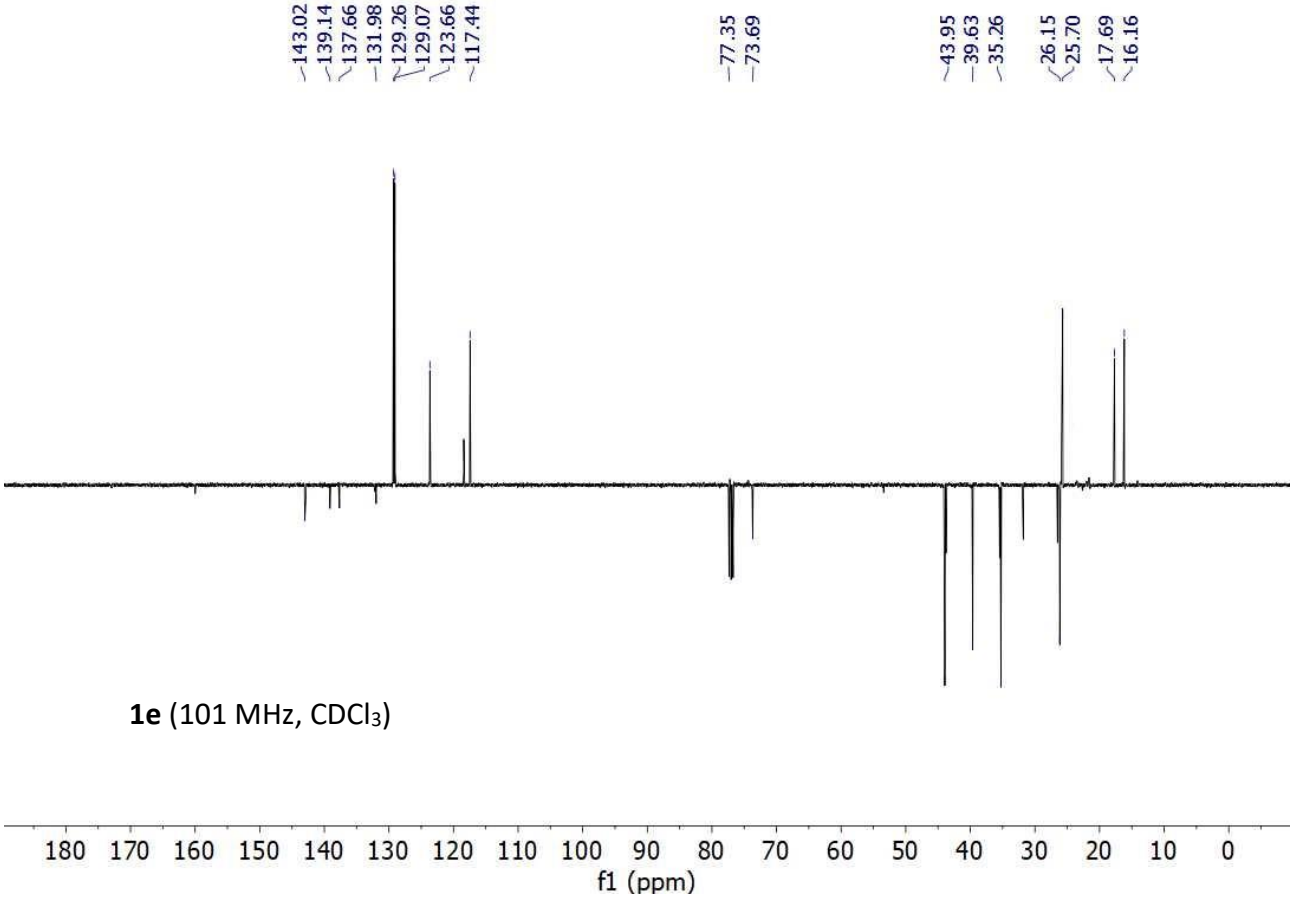

1e (101 MHz, $CDCl_3$)

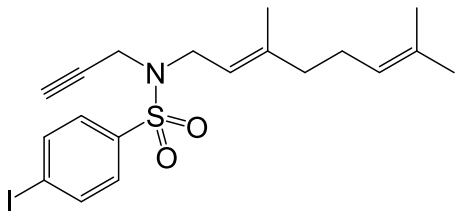

1f (400 MHz, $CDCl_3$)

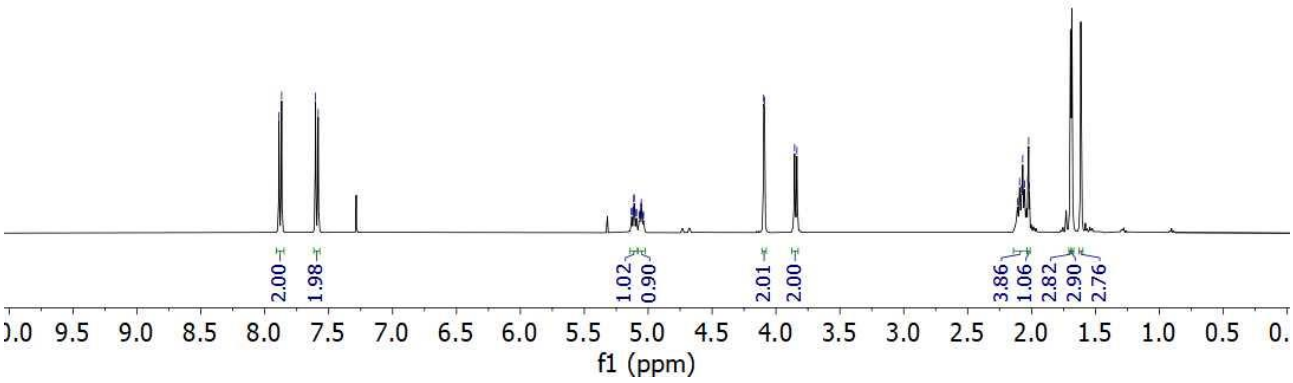

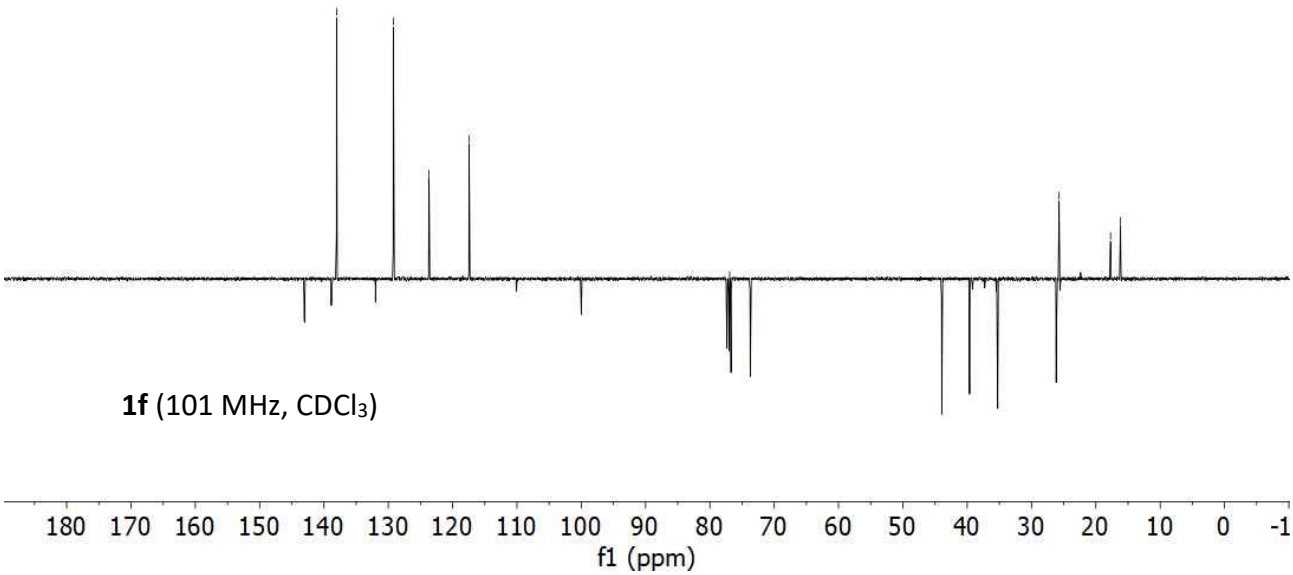

1f (101 MHz, $CDCl_3$)

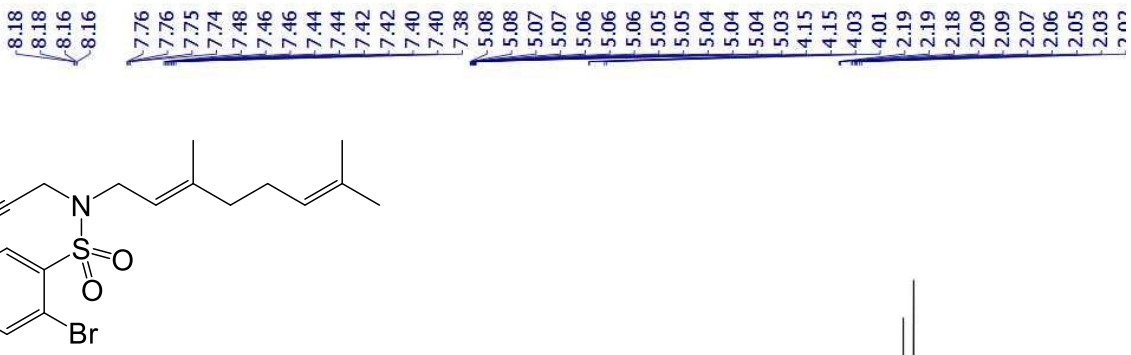

1g (400 MHz, $CDCl_3$)

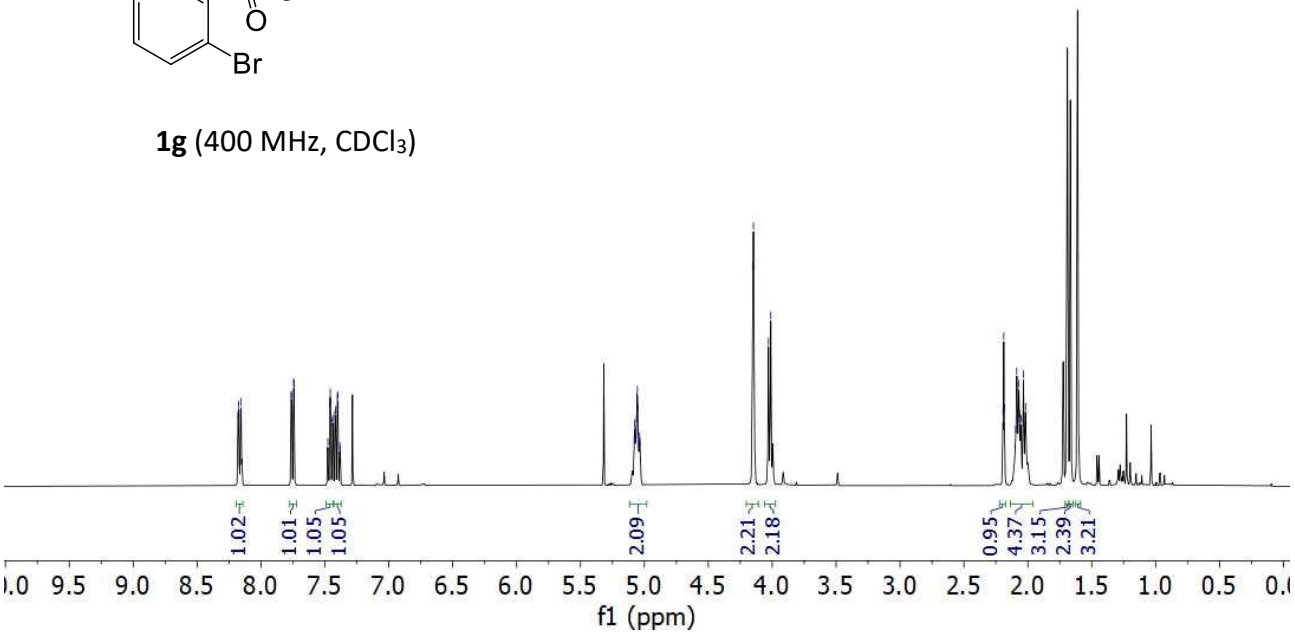

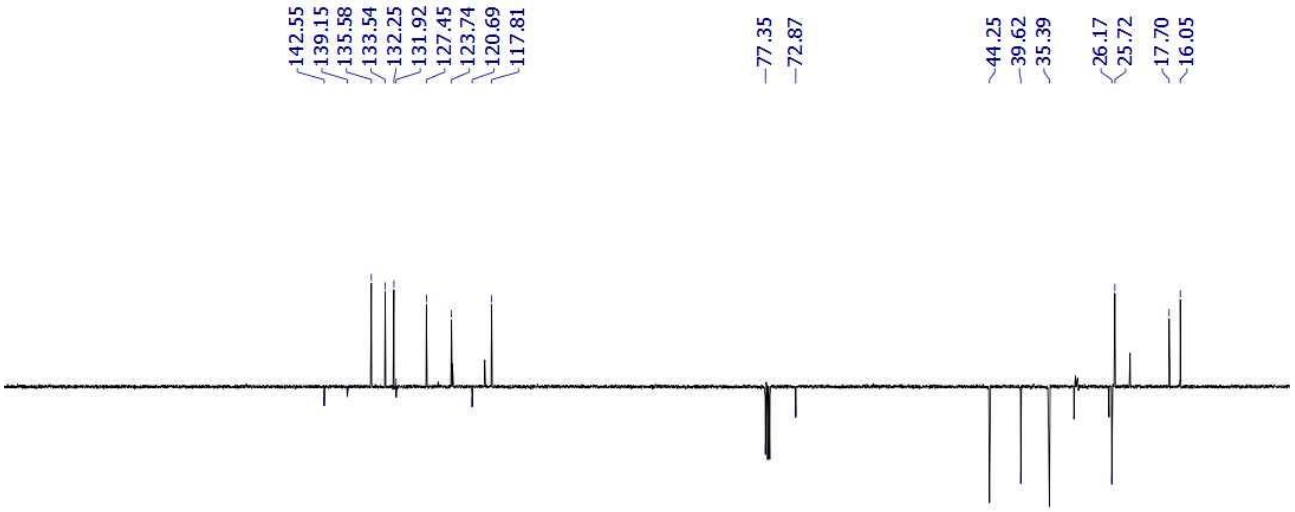

1g (101 MHz, $CDCl_3$)

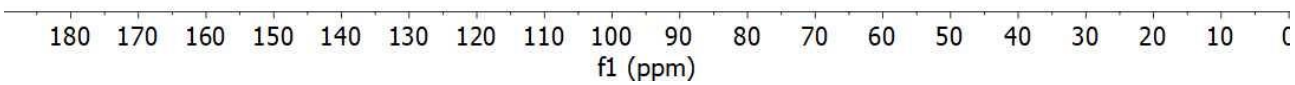

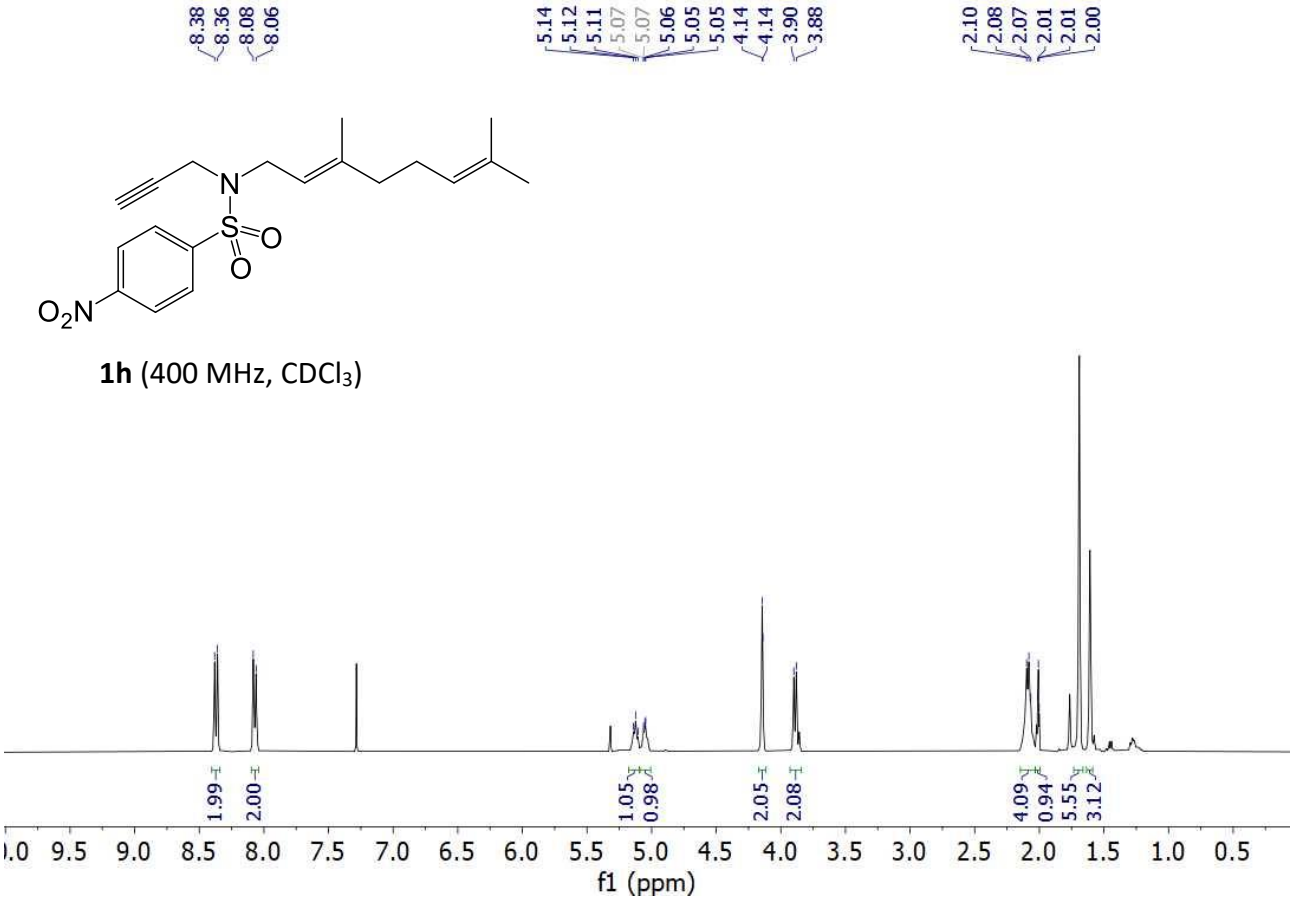

1h (400 MHz, $CDCl_3$)

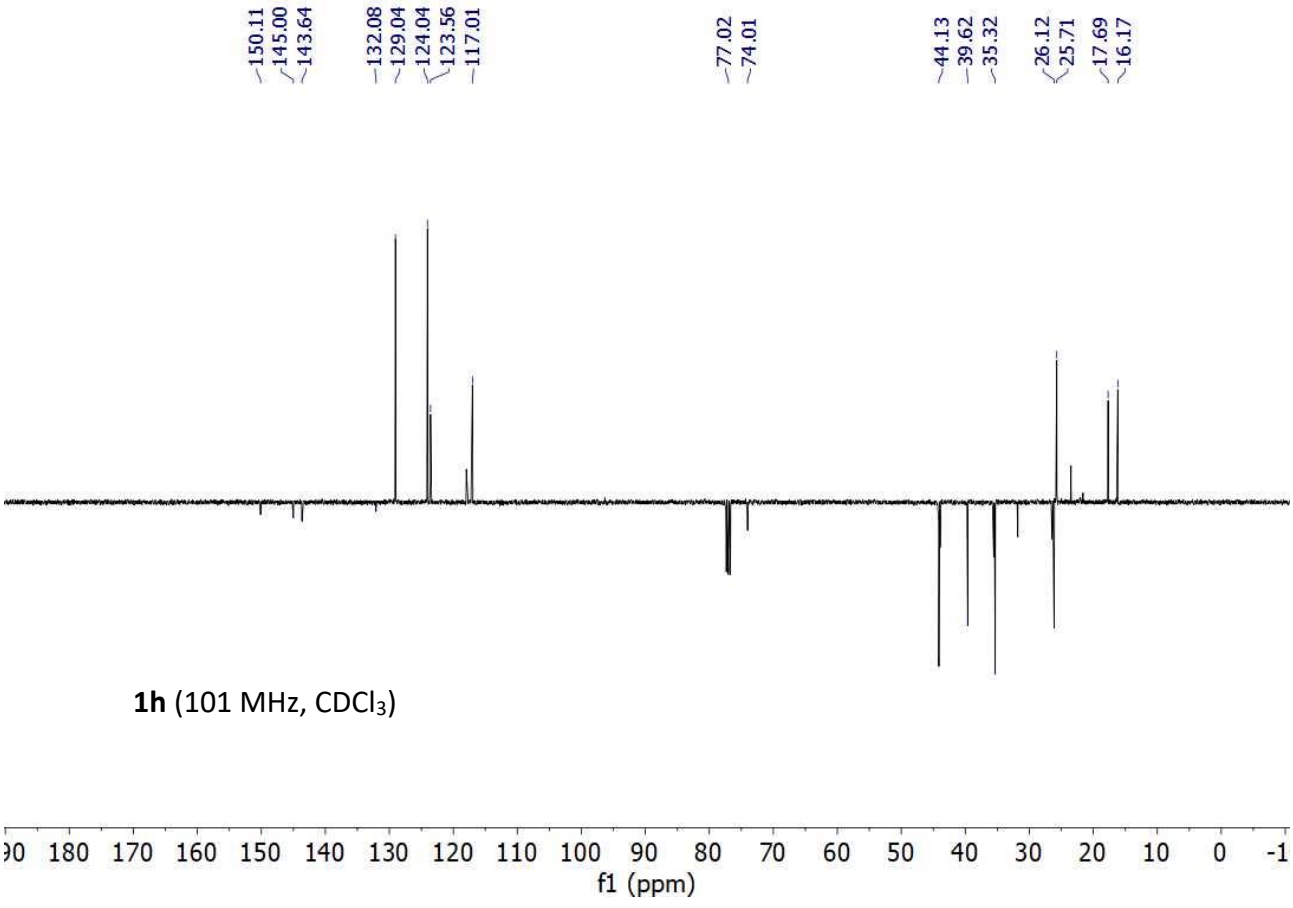

1h (101 MHz, $CDCl_3$)

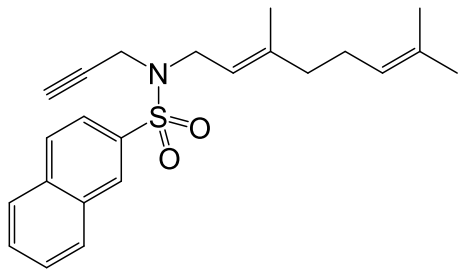

1i (400 MHz, $CDCl_3$)

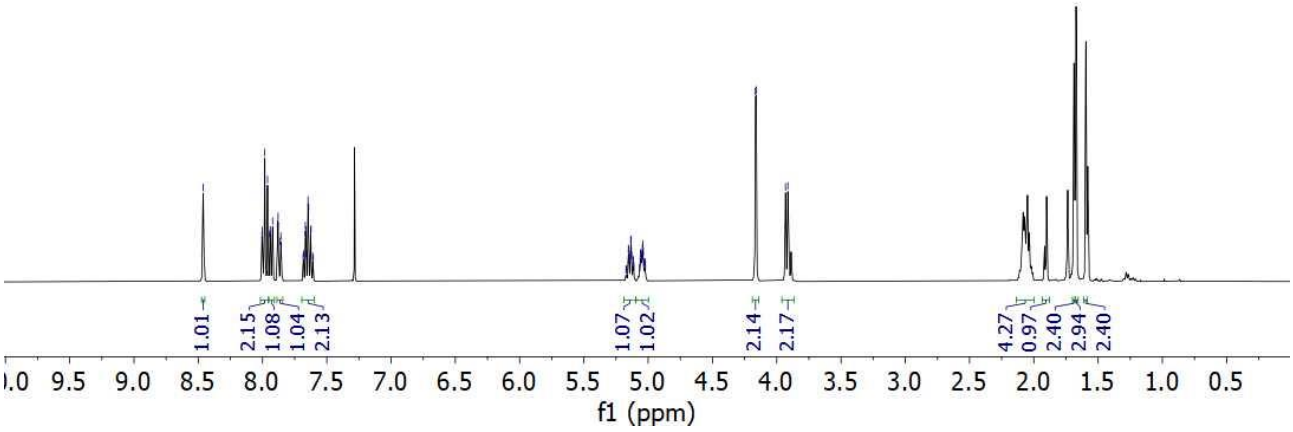

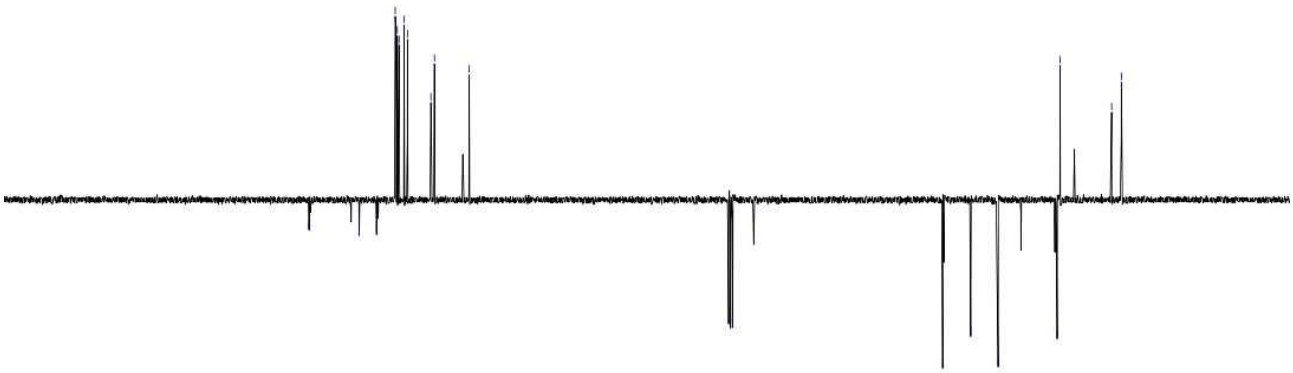

1i (101 MHz, $CDCl_3$)

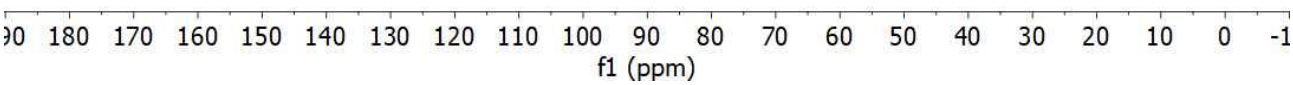

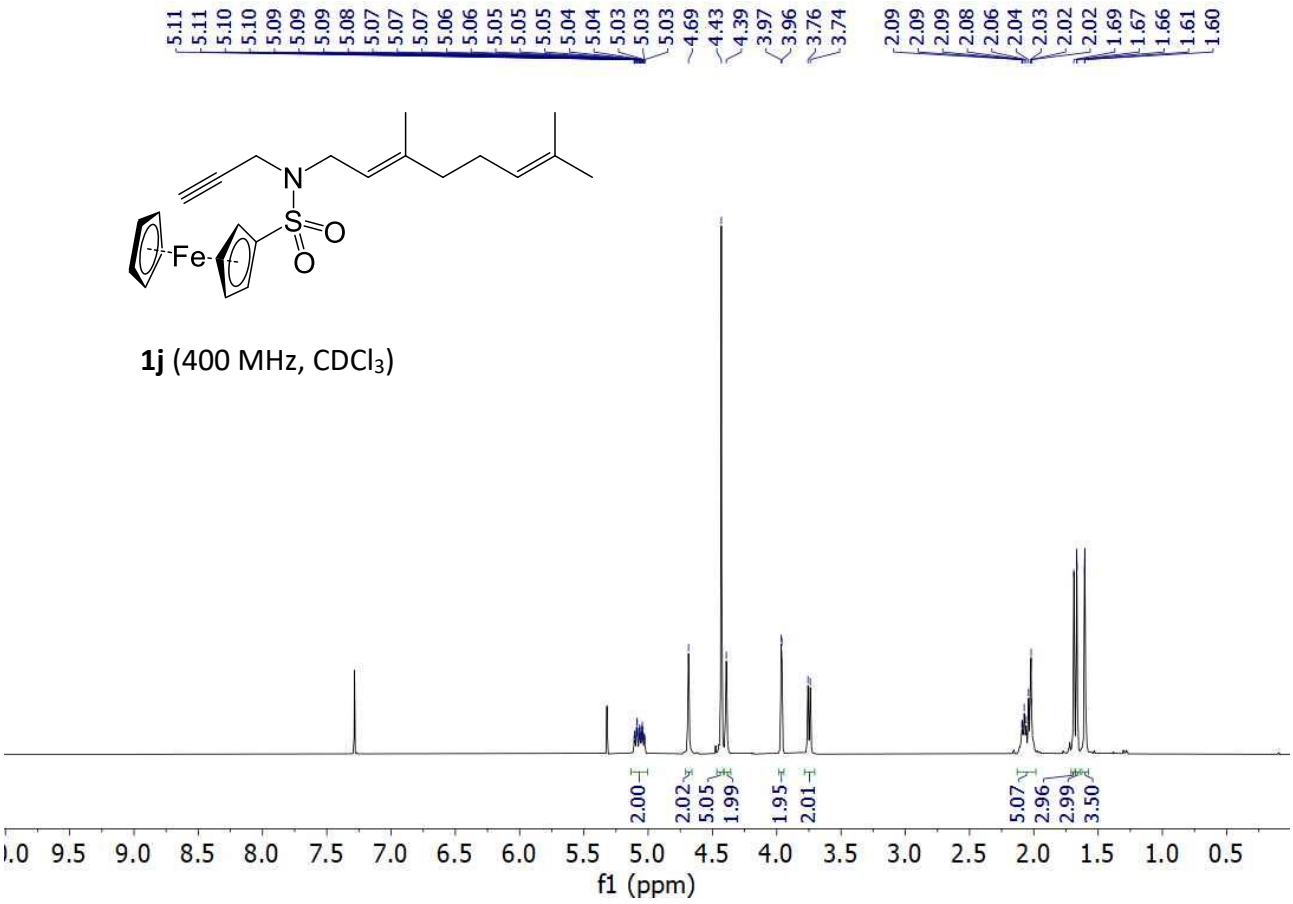

1j (400 MHz, $CDCl_3$)

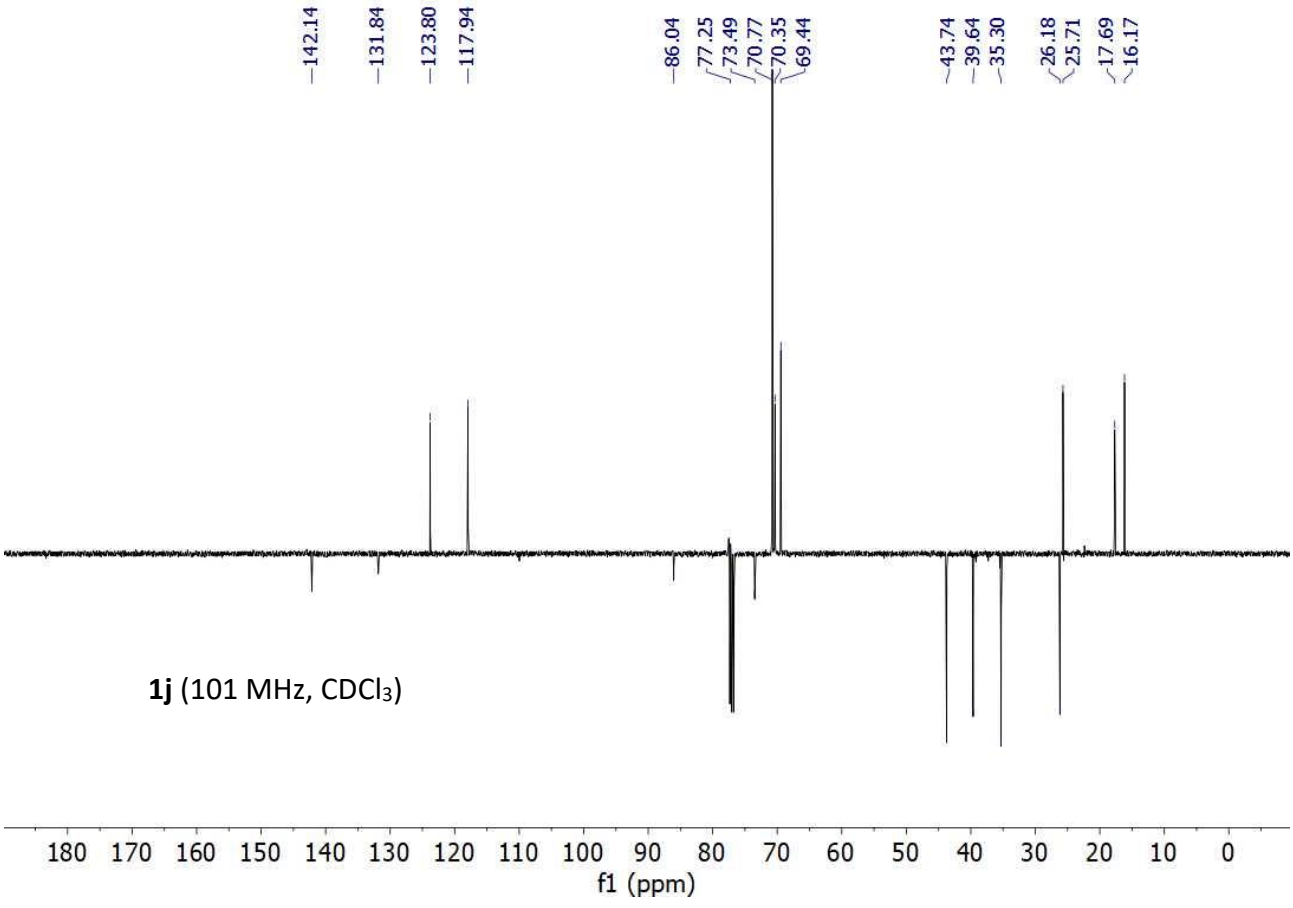

1j (101 MHz, $CDCl_3$)

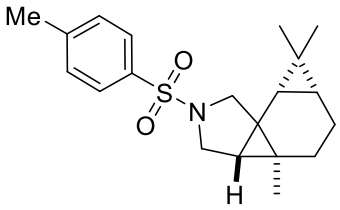

2b (400 MHz, $CDCl_3$)

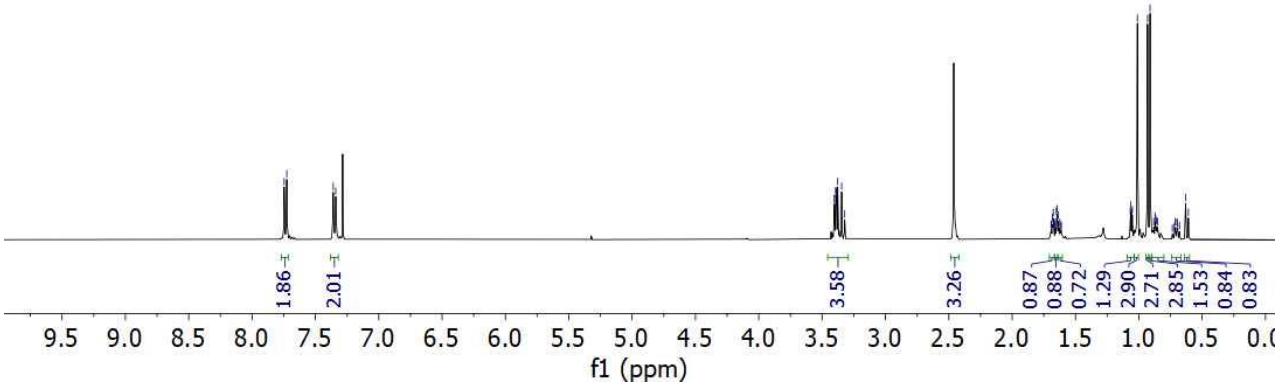

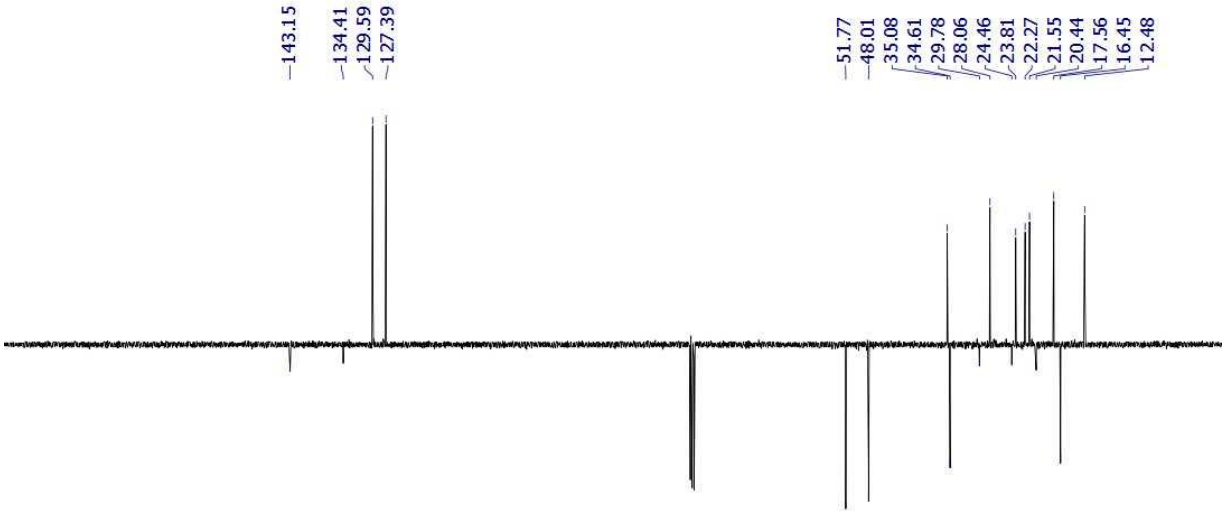

2b (101 MHz, $CDCl_3$)

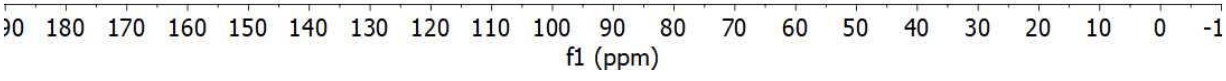

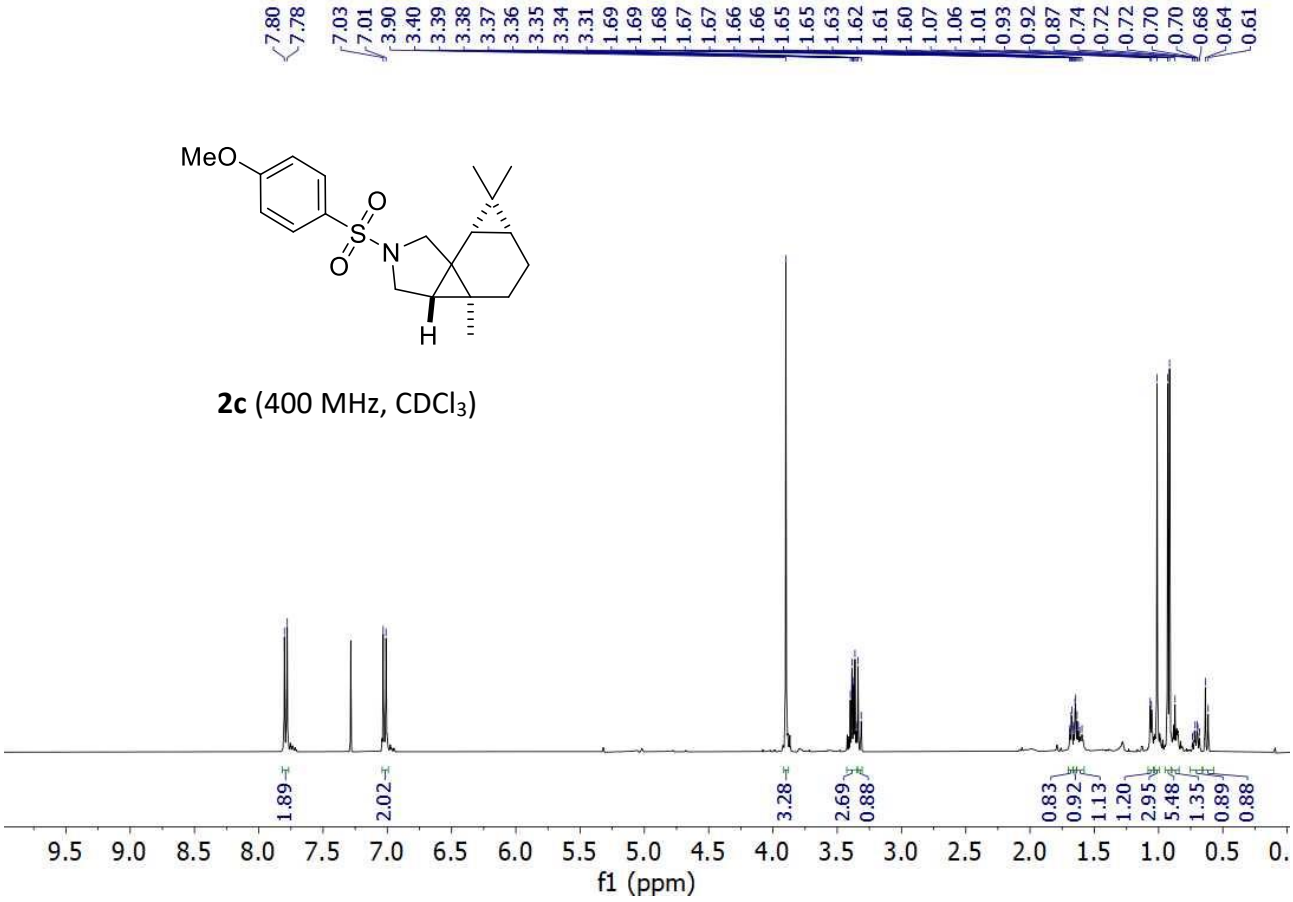

2c (400 MHz, $CDCl_3$)

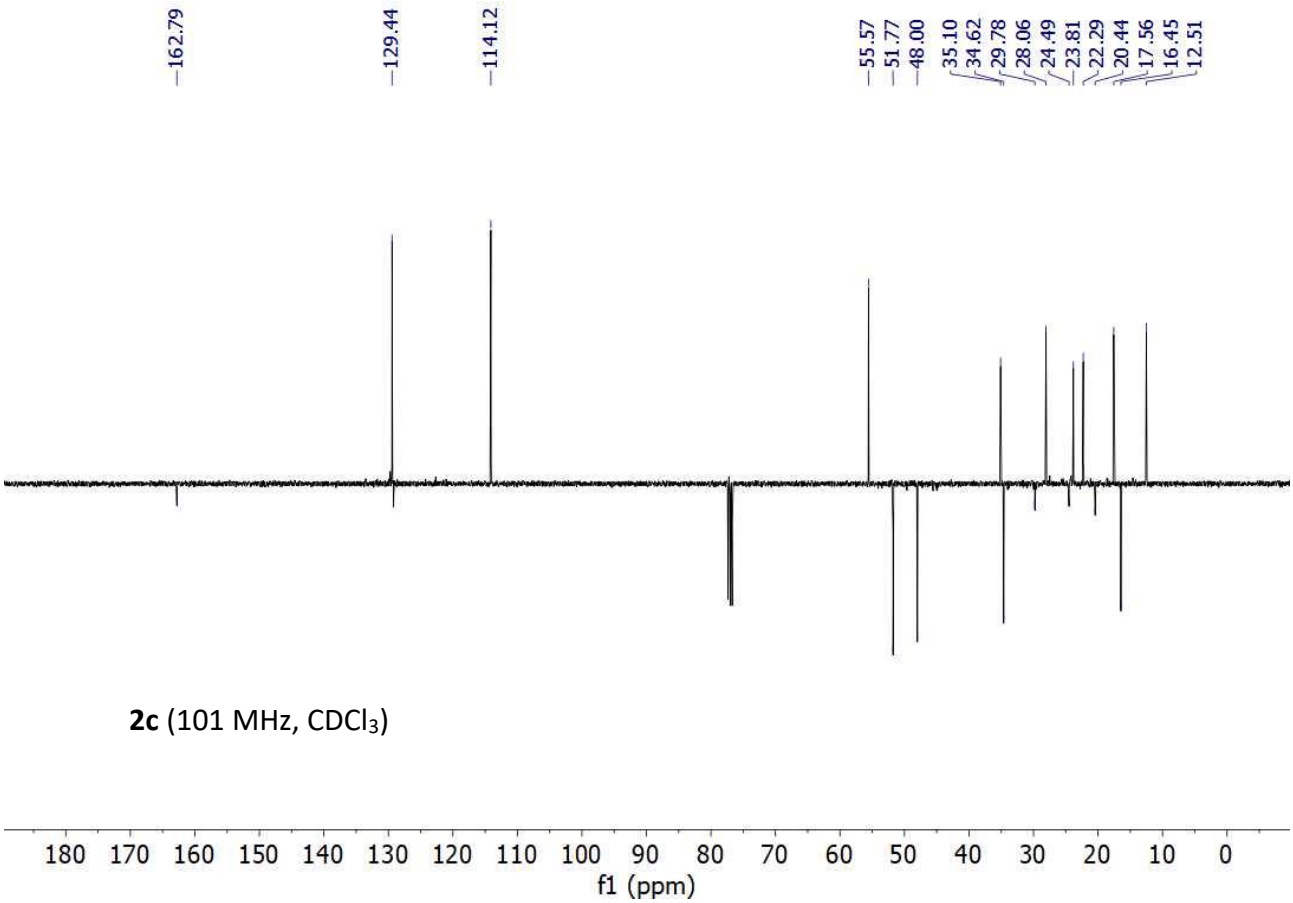

2c (101 MHz, $CDCl_3$)

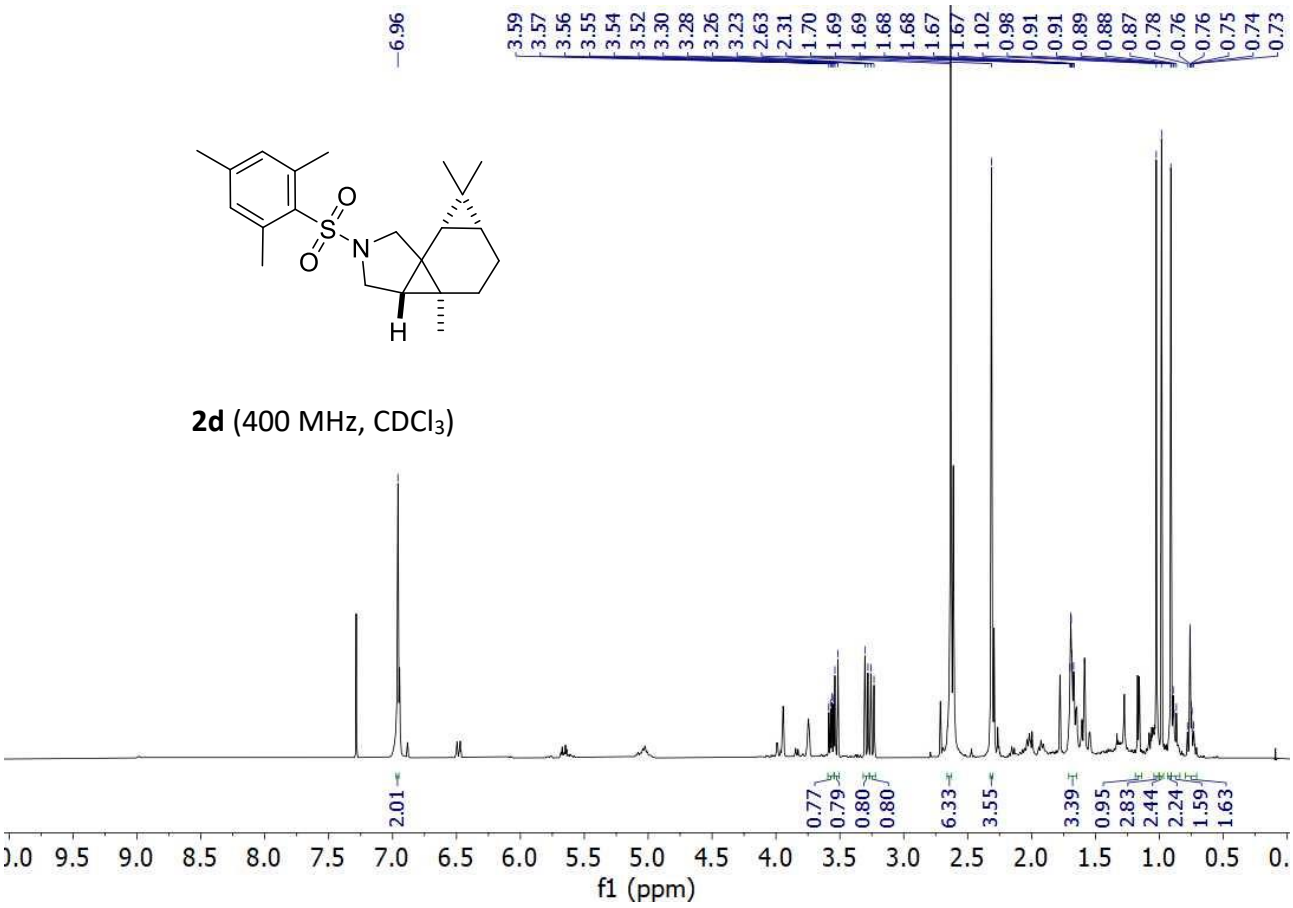

2d (400 MHz, $CDCl_3$)

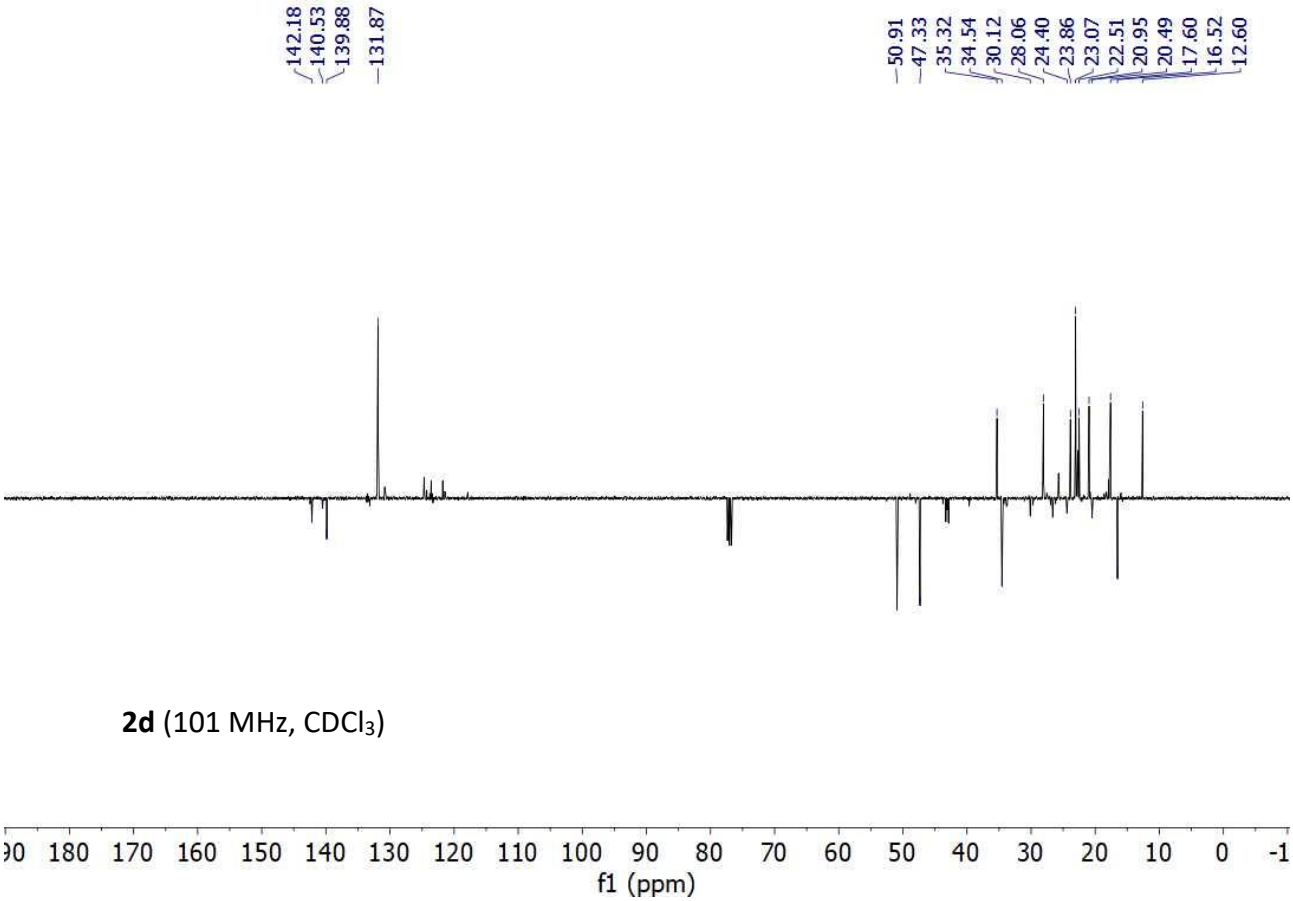

2d (101 MHz, $CDCl_3$)

2e (400 MHz, $CDCl_3$)

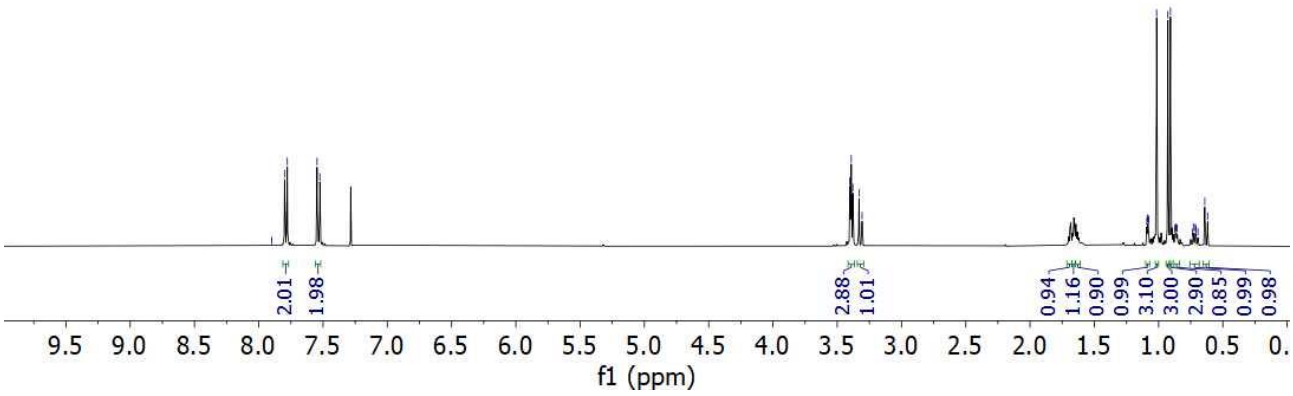

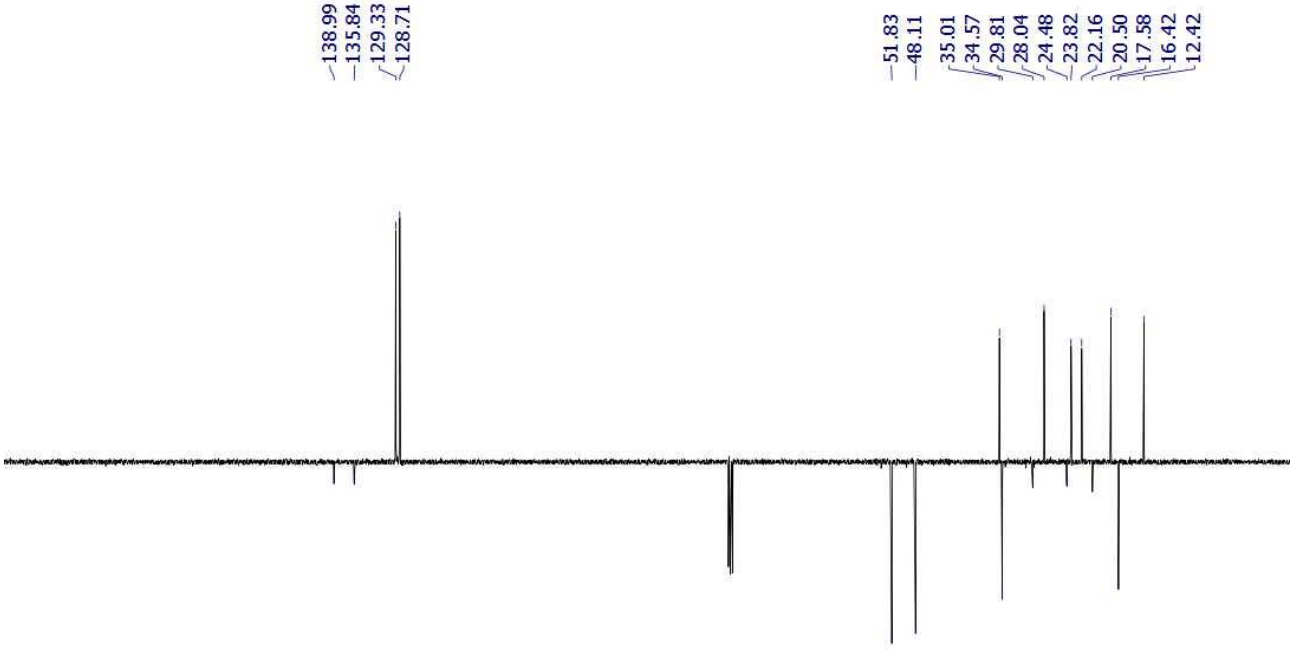

2e (101 MHz, $CDCl_3$)

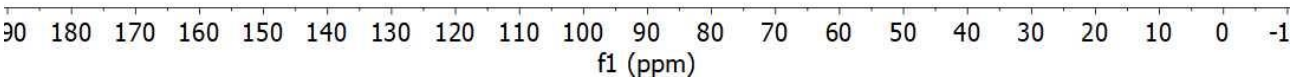

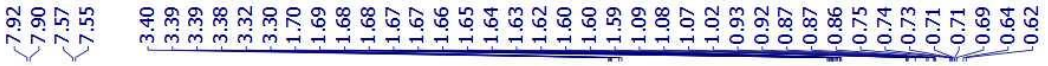

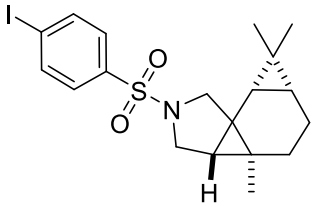

2f (400 MHz, $CDCl_3$)

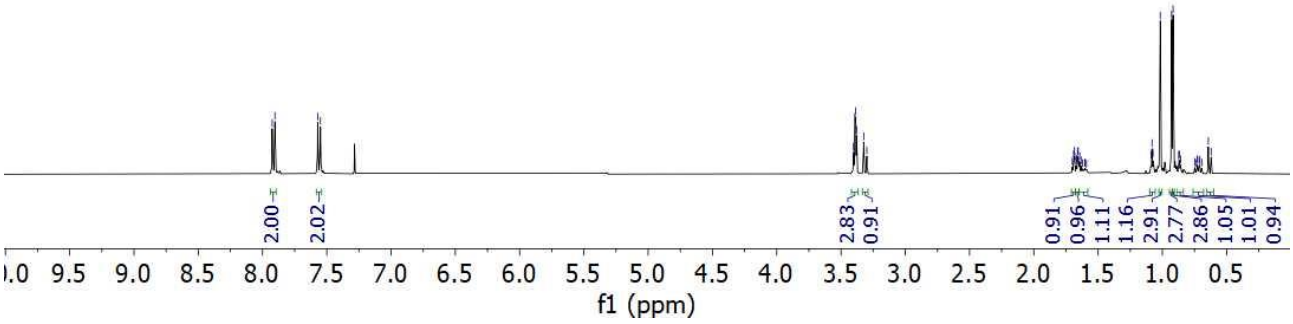

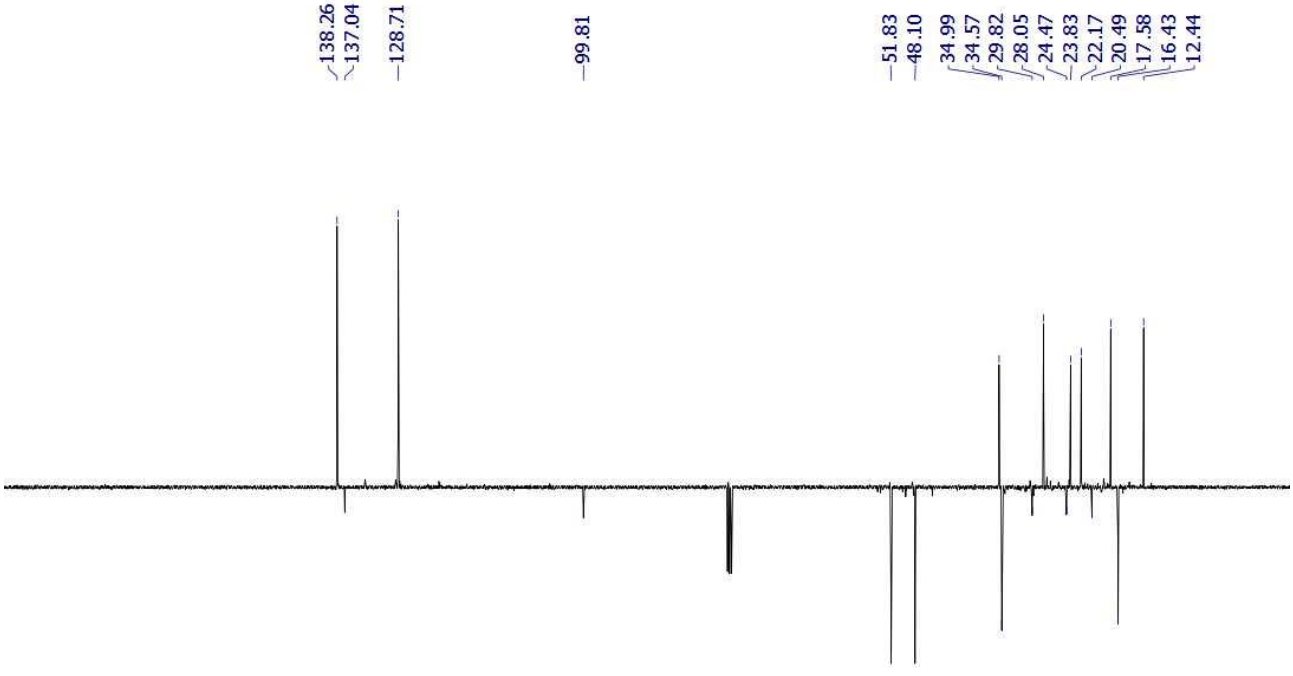

2f (101 MHz, $CDCl_3$)

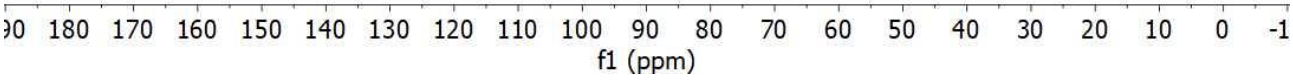

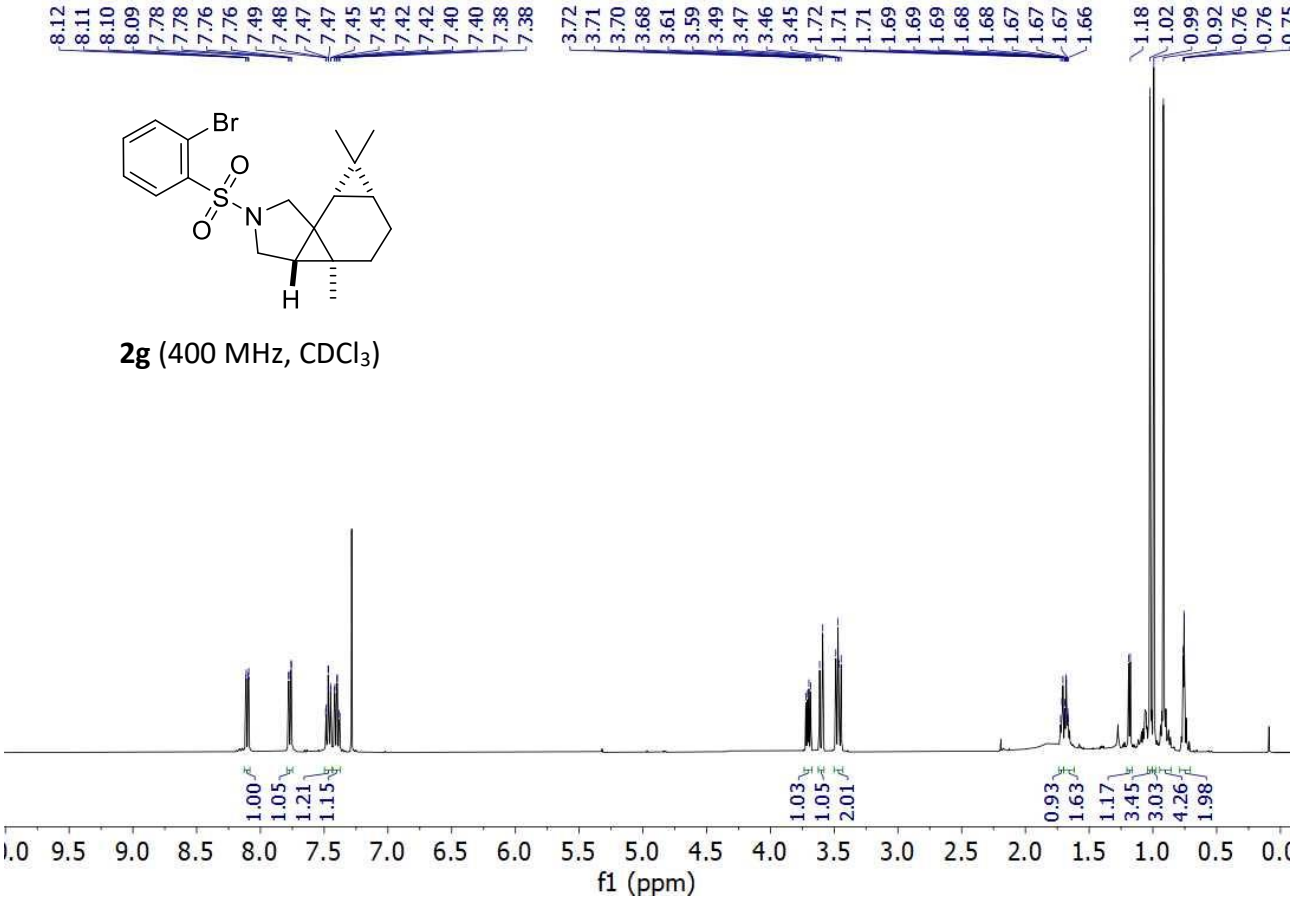

2g (400 MHz, $CDCl_3$)

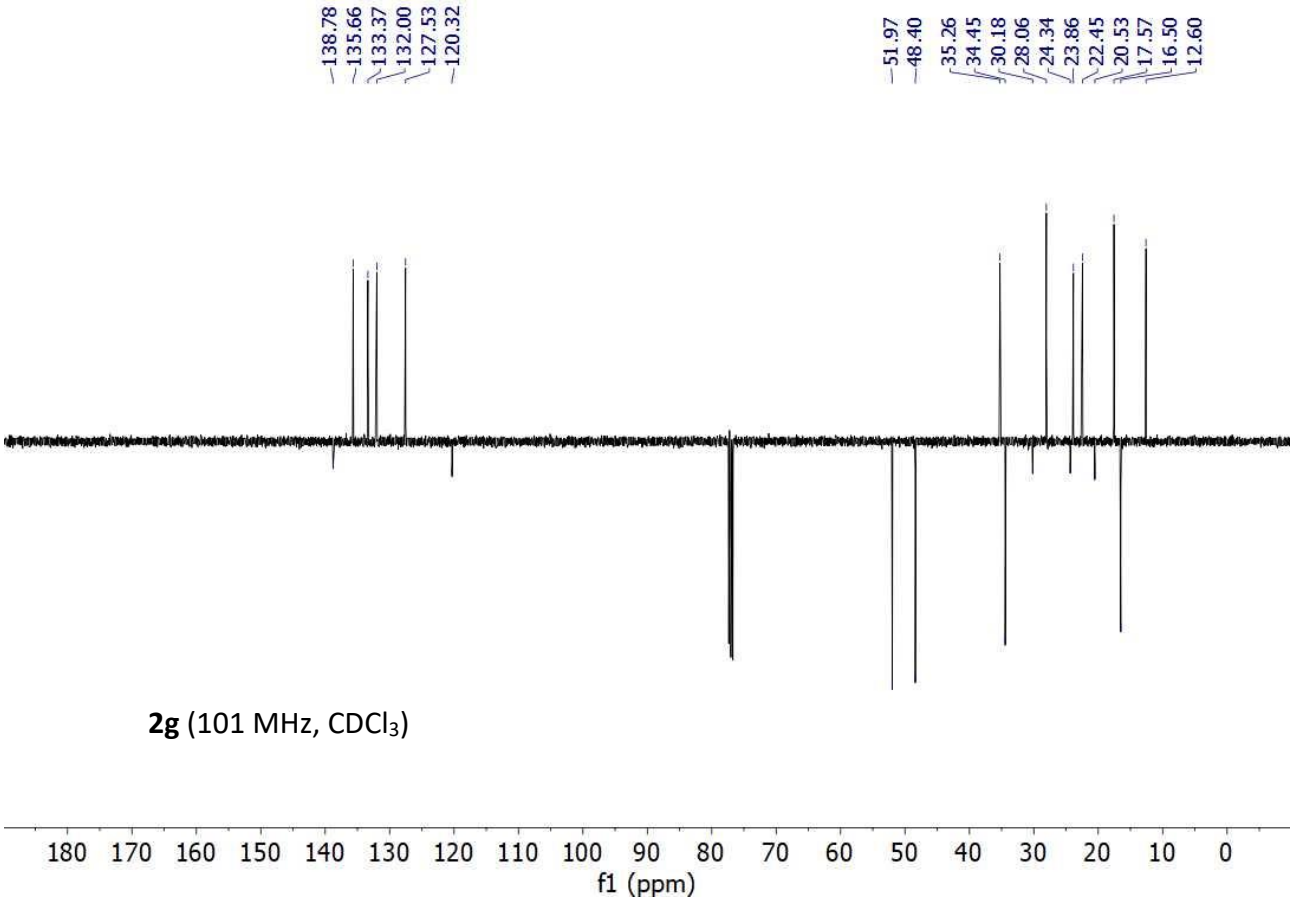

2g (101 MHz, $CDCl_3$)

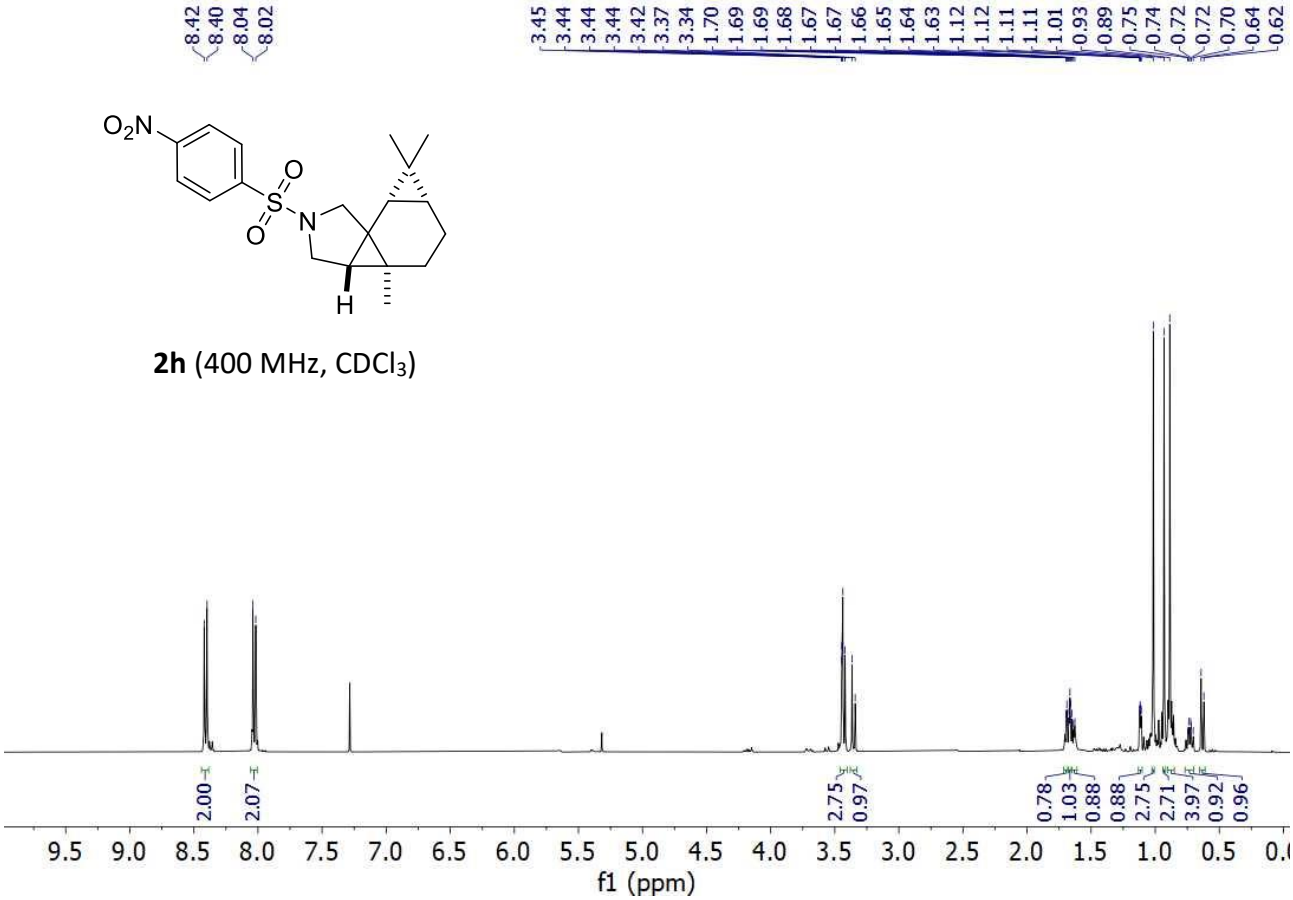

2h (400 MHz, $CDCl_3$)

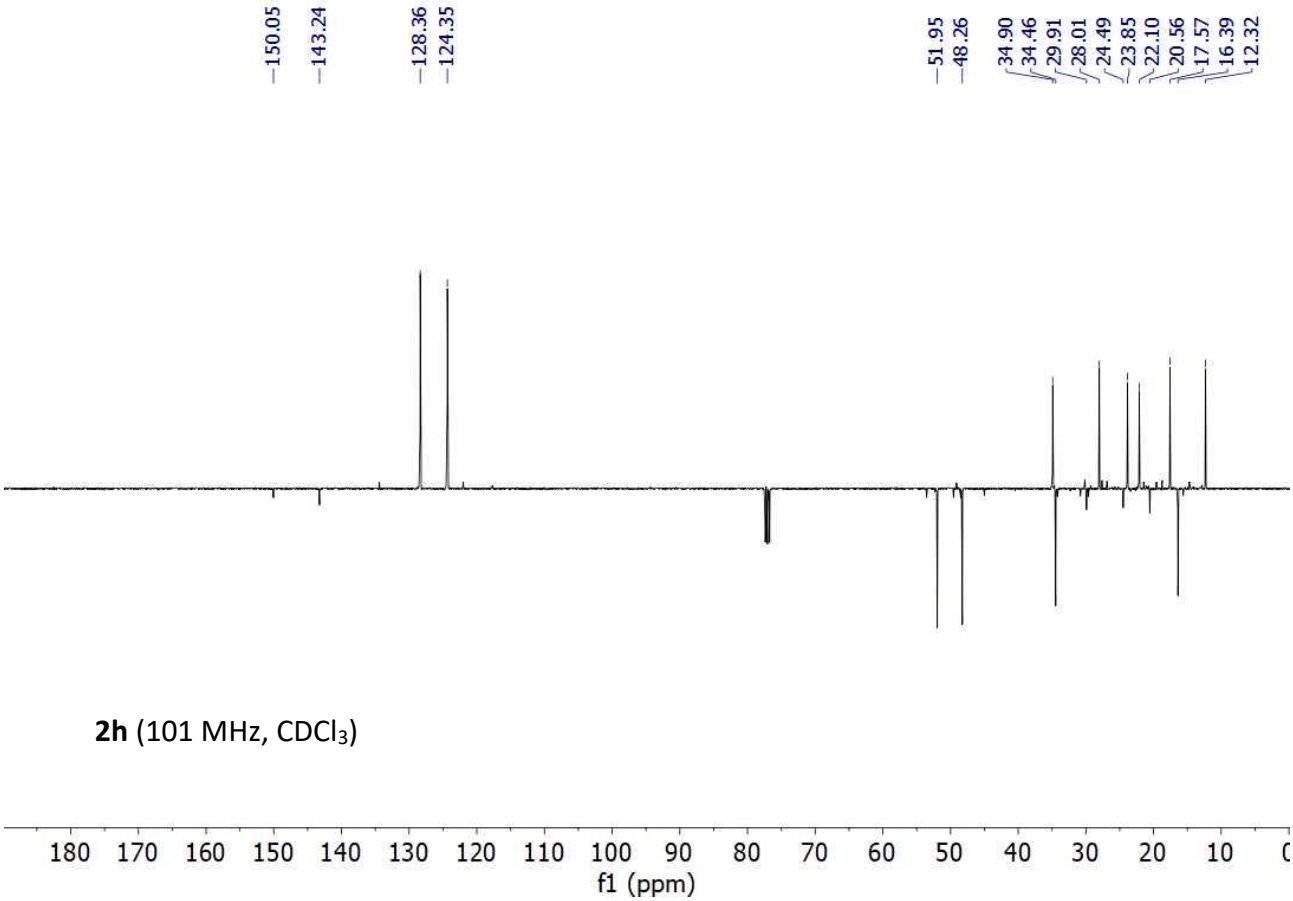

2h (101 MHz, $CDCl_3$)

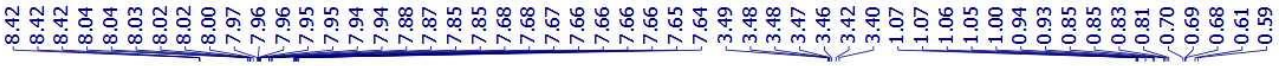

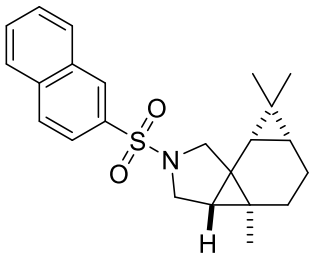

2i (400 MHz, $CDCl_3$)

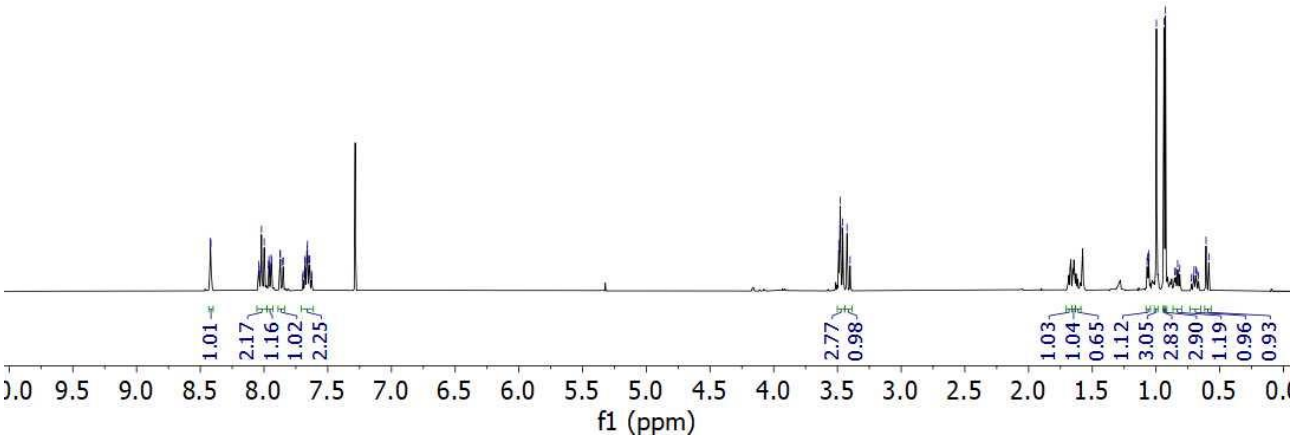

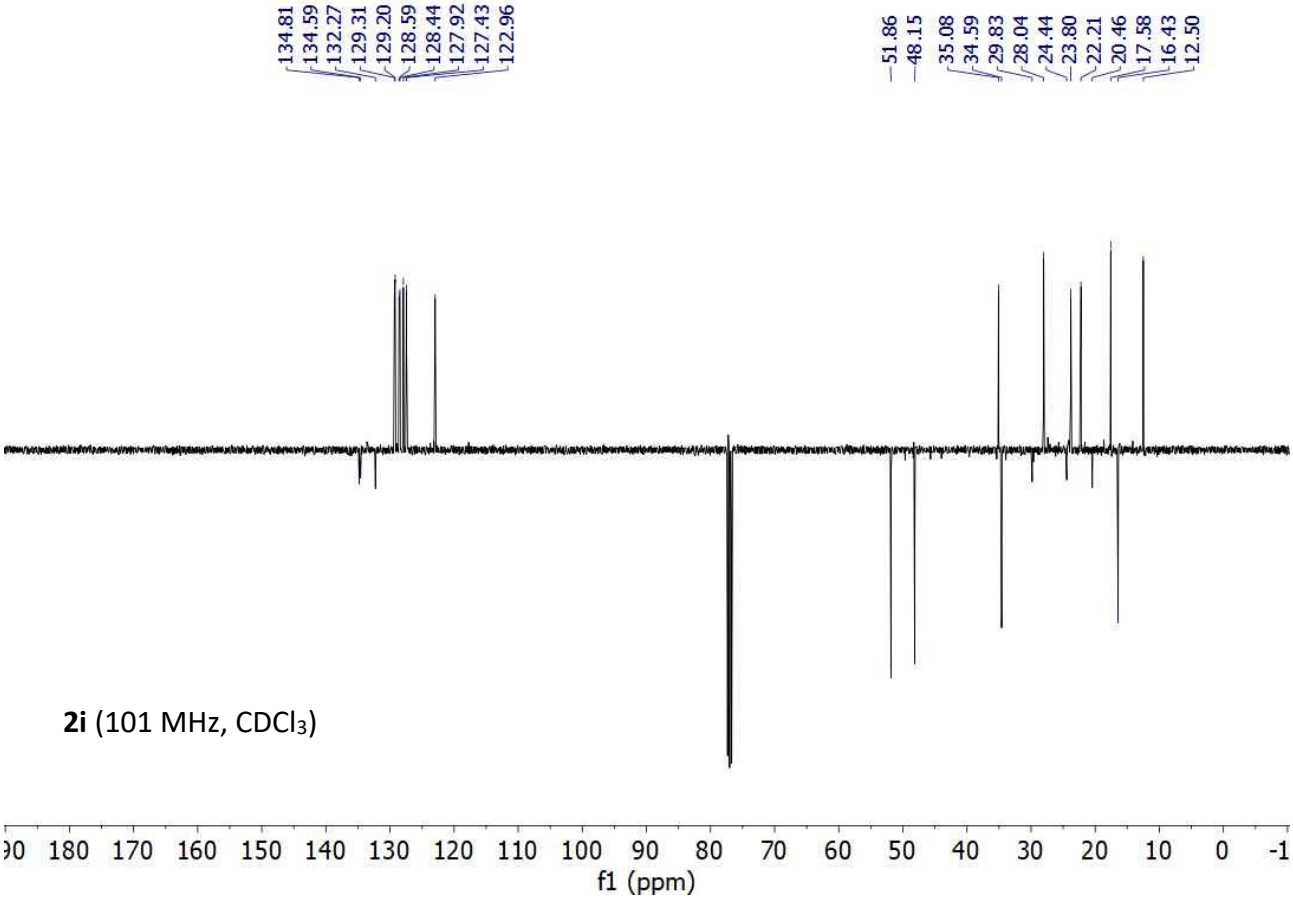

2i (101 MHz, $CDCl_3$)

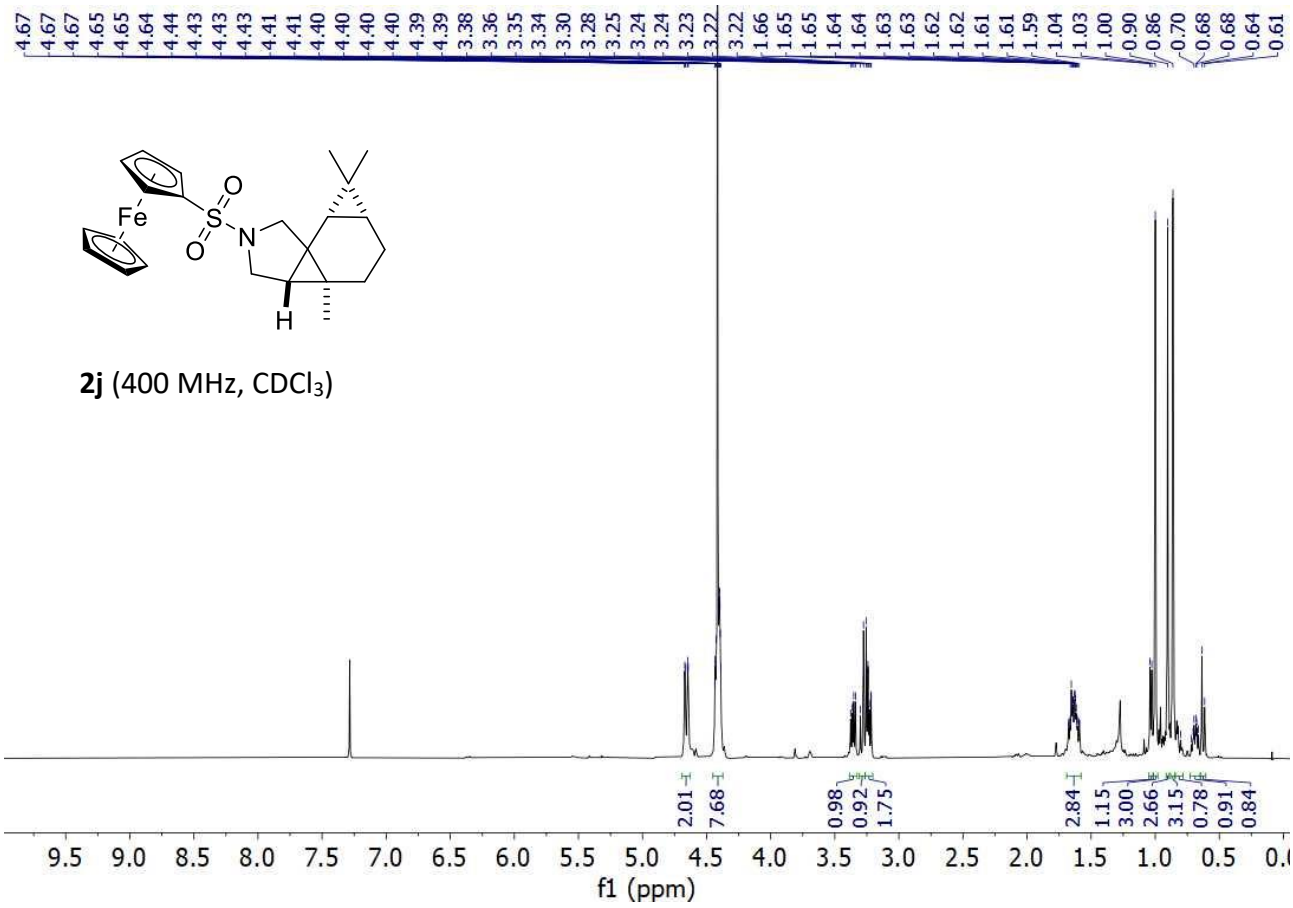

2j (400 MHz, $CDCl_3$)

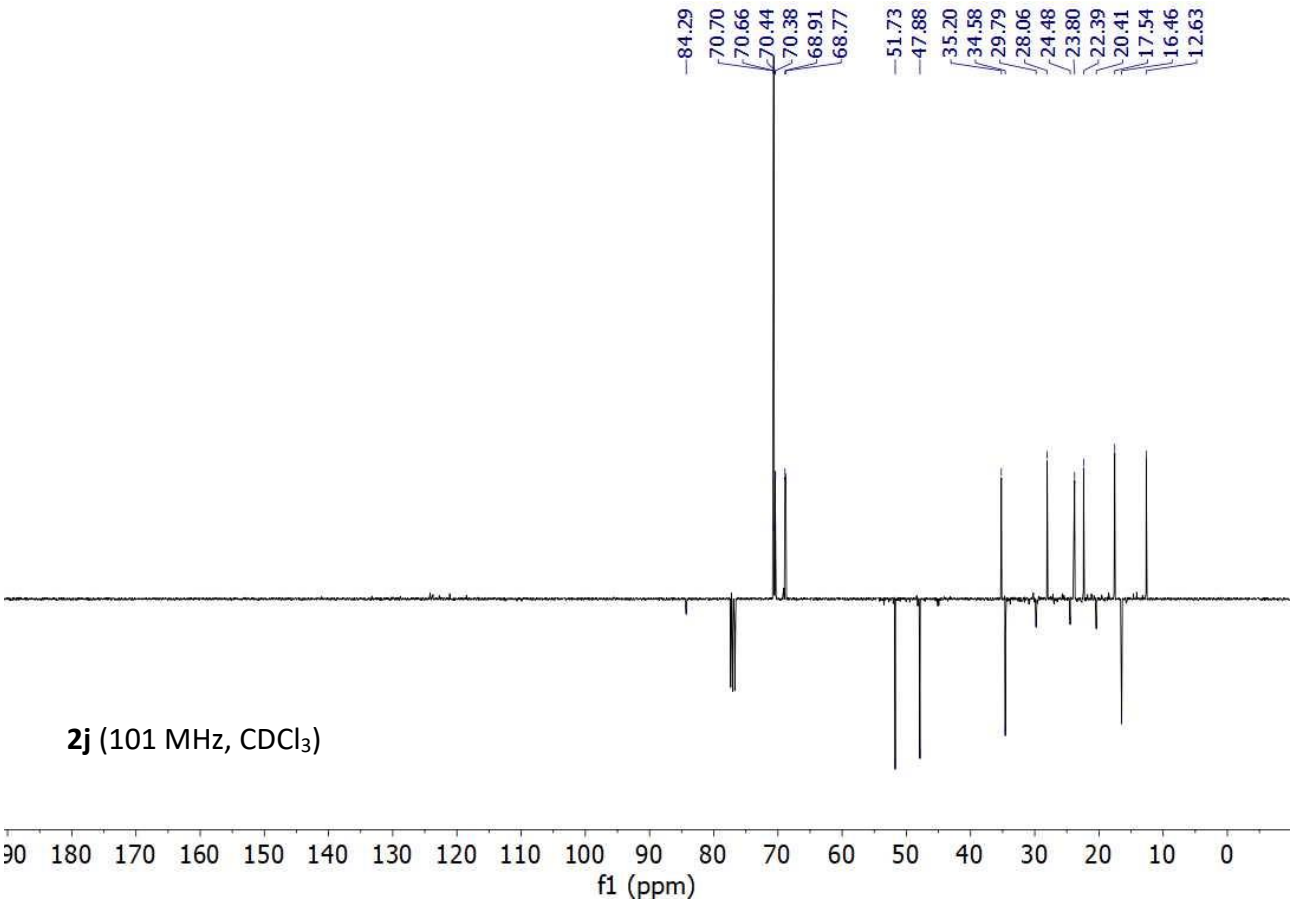

2j (101 MHz, $CDCl_3$)

- **References**

1) a) X. Zhang, Q. Zhang, L. Li, S. Cao, Z. Liu, G. Zanoni, Y. Ning and Y. Wu, *Org. Lett.*, 2021, **23**, 3674; b) M. Gao, Q. Gao, X. Hao, Y. Wu, Q. Zhang, G. Liu and R. Liu, *Org. Lett.* 2020., **22**, 3, 1139.ù

2) G. Giovanardi, A. Secchi, A. Arduini and G. Cera, *Beilstein J. Org. Chem.*, 2022, **18**, 190.

3) 3) C. Nieto-Oberhuber, S. Lopéz, M. Paz Mŭnoz, E. Jiménez-Núñez, E. Buñuel, D. J. Cárdenas and A. M. Echavarren, *Chem. –Eur. J.*, 2006, **12**, 1694.